mathematics

MDPI

Article

Feedback Tracking Constraint Relaxation Algorithm for Constrained Multi-Objective Optimization

Yuling Lai [1], Junming Chen [2], Yile Chen [2], Hui Zeng [3] and Jialin Cai [1,*]

[1] School of Art and Design, Guangzhou University, Guangzhou 510006, China; laiyuling1102@gzhu.edu.cn
[2] Faculty of Humanities and Arts, Macau University of Science and Technology, Macao 999078, China; jmchen@must.edu.mo (J.C.); chenyile@must.edu.mo (Y.C.)
[3] School of Design, Jiangnan University, Wuxi 214122, China; 7230306023@stu.jiangnan.edu.cn
* Correspondence: jialin@gzhu.edu.cn

Abstract: In practical applications, constrained multi-objective optimization problems (CMOPs) often fail to achieve the desired results when dealing with CMOPs with different characteristics. Therefore, to address this drawback, we designed a constraint multi-objective evolutionary algorithm based on feedback tracking constraint relaxation, referred to as CMOEA-FTR. The entire search process of the algorithm is divided into two stages: In the first stage, the constraint boundaries are adaptively adjusted based on the feedback information from the population solutions, guiding the boundary solutions towards neighboring solutions and tracking high-quality solutions to obtain the complete feasible region, thereby promoting the population to approach the unconstrained Pareto front (UPF). The obtained feasible solutions are stored in an archive and continuously updated to promote the diversity and convergence of the population. In the second stage, the scaling of constraint boundaries is stopped, and a new dominance criterion is established to obtain high-quality parents, thereby achieving the complete constrained Pareto front (CPF). Additionally, we customized an elite mating pool selection, an archive updating strategy, and an elite environmental selection truncation mechanism to maintain a balance between diversity and convergence. To validate the performance of CMOEA-FTR, we conducted comparative experiments on 44 benchmark test problems and 16 real-world application cases. The statistical IGD and HV metrics indicate that CMOEA-FTR outperforms seven other CMOEAs.

Keywords: constrained multi-objective optimization; evolutionary algorithm; feedback tracking; archive

MSC: 68w50; 90c29; 49k99

check for updates

Academic Editor: Víctor Yepes

Received: 12 January 2025
Revised: 2 February 2025
Accepted: 12 February 2025
Published: 14 February 2025

Citation: Lai, Y.; Chen, J.; Chen, Y.; Zeng, H.; Cai, J. Feedback Tracking Constraint Relaxation Algorithm for Constrained Multi-Objective Optimization. *Mathematics* **2025**, *13*, 629. https://doi.org/10.3390/math13040629

Copyright: © 2025 by the authors. Licensee MDPI, Basel, Switzerland. This article is an open access article distributed under the terms and conditions of the Creative Commons Attribution (CC BY) license (https://creativecommons.org/licenses/by/4.0/).

1. Introduction

To handle constrained multi-objective optimization problems (CMOPs) [1] more effectively, researchers have integrated CMOPs into many practical applications, such as micro-grid dispatch with frequency dynamics [2], refined oil distribution [3], and distribution network stochastic reconfiguration [4]. Xia et al. [5] proposed a meta-learning-based alternating minimization (MLAM) method to solve non-convex optimization. Nowdeh et al. [6] proposed a gray wolf optimizer to prevent it from getting trapped in local optima, thereby reducing energy generation losses. The mathematical formulation of a CMOP is defined as follows:

$$\begin{aligned} &\text{Minimize } F(x) = (f_1(x), \cdots, f_m(x)) \\ &\text{Subject to } g_i(x) \leq 0, i = 1, \cdots, p \\ &\qquad\qquad h_j(x) = 0, j = p+1, \cdots, q \\ &\qquad\qquad x \in \Omega \end{aligned} \tag{1}$$

Here, $f_m(x)$ represents the m-th objective function, while $g_i(x)$ and $h_j(x)$ denote the inequality constraints and equality constraints, respectively. To differentiate the constraint satisfaction capability of solutions, it is often necessary to calculate the constraint violation degree of each solution for each objective function. The calculation of constraint violation degree is as follows:

$$CV_j(x) = \begin{cases} \max(0, g_j(x)), & j = 1, \cdots, p \\ \max(0, |h_j(x)| - \delta), & j = p+1, \cdots, q \end{cases} \tag{2}$$

In the formula, δ is a positive tolerance parameter, which is set to ing10^{-6} in this paper. Its primary function is to convert equality constraints into inequality constraints, thereby calculating the constraint violation degree of each solution for each objective function. To determine the dominance relationship between solutions, it is necessary to calculate the total constraint violation degree of each solution. The specific mathematical definition is as follows:

$$CV(x) = \sum_{j=1}^{q} CV_j(x) \tag{3}$$

To handle CMOPs more effectively, researchers have proposed various types of constraint handling techniques. For example, the two-stage archiving framework of C-TSEA [7], the dual-population cooperative evolution framework of CCMO [8], and the dual-archive cooperative evolution concept of C-TAEA [9] have been put forward. Although multi-objective evolutionary algorithms (MOEAs) [10] have made significant progress over the past two decades, they still fail to achieve the desired results when faced with conflicts between multiple objectives and constraints. To address this challenge, researchers have improved constraint handling techniques based on existing technologies. Tian et al. proposed CMOEA-MS [11], which involves adaptively adjusting objectives and constraints based on fitness evaluation metrics. Wang et al. [12] proposed a method to handle conflicts between objectives and constraints more effectively by dividing the main population into m subpopulations. The archive population and the m subpopulations undergo cooperative evolution across the entire objective space to obtain a complete feasible region.

Additionally, many researchers have introduced the concept of temporary archives to preserve high-quality solutions during the evolutionary process. As the algorithm evolves, the archive is continuously updated. For example, Li et al. [13] proposed a dual-archive cooperative evolution framework named CMOEA-TWC, which primarily utilizes weak cooperation between archives to enhance the algorithm's search performance. The C-TSEA [7] algorithm proposed by Tian et al. utilizes collaboration between the archive and the population to improve the algorithm's performance.

Although the aforementioned improvements in MOEAs have significantly enhanced algorithm performance, algorithms often struggle to search all feasible regions, particularly when dealing with discontinuous and narrow feasible regions, and are highly likely to become trapped in local optima. To enable the algorithm to traverse infeasible regions and obtain a complete CPF, a CMOEA based on feedback tracking constraint relaxation is proposed to address the shortcomings of the aforementioned algorithms. The main contributions of this paper are as follows:

(1) A novel two-stage archiving framework is employed. Stage One: To obtain more information about solutions, a boundary constraint learning mechanism that adaptively adjusts based on constraint violation degree and fitness is designed. This mechanism drives solutions within the boundaries to explore neighboring solutions, encouraging the population to approach the CPF. Feasible solutions are stored in the archive, and redundant solutions are removed based on fitness ranking. Stage Two: The principle of constraint scaling is stopped, and high-quality solutions are tracked to obtain high-quality parents, ensuring the convergence of the population. During the elite environmental selection process, redundant solutions are removed based on objective value sorting and diversity ranking to ensure the diversity of the algorithm.
(2) In the parent selection for the mating pool process, a strict secondary dominance principle strategy is designed. Building upon existing constraint dominance principles, non-dominance is determined based on constraint relaxation values, and density is added as an indicator for the secondary dominance principle of solutions, to ensure the convergence and feasibility of the algorithm.
(3) A new fitness evaluation strategy is designed for updating the archive and removing solutions within constraint boundaries. Ranking rules for diversity and convergence are added to the standard fitness strategy to obtain more information about solutions and enhance the convergence of the population.

The remainder of this paper is organized as follows: Section 2 discusses related work and motivation. Section 3 provides a detailed explanation of the proposed CMOEA-FTR. Section 4 presents experimental studies and validation. Finally, Section 5 summarizes the research and outlines future directions.

2. Related Work and Motivations

In this chapter, relevant related work is analyzed, and the motivation behind this work is explained, thereby supporting the strong competitiveness of CMOEA-FTP.

2.1. Related Work

Through researchers' persistent efforts, existing CMOEAs [14] have made significant progress in search capabilities. Generally, CMOEAs can be roughly classified into the following three categories based on the priority of constraints and objectives.

(1) First category: Constraints have a higher priority than objectives. Researchers tend to prioritize constraints during the search process of the algorithm. In the algorithm search process described in [15], all infeasible solutions that arise are discarded. Unfortunately, when most of the solutions are infeasible, the algorithm loses selection pressure, significantly reducing both its diversity and convergence. To address this issue, Deb designed an algorithm based on the constraint dominance principle, named NSGA-II-CDP [16]. The purpose of the constraint dominance principle is to generate higher-quality solutions. To further enhance the algorithm's selection pressure on solutions, ref. [17] extends this theory by incorporating solutions with lower constraint violations into the population. Recently, researchers have considered the total constraint violation degree of solutions. In [18], infeasible solutions with lower total constraint violations are selected as candidate solutions to increase the algorithm's diversity. To further enhance the overall performance of the algorithm, researchers have embedded the constraint dominance principle into the framework of decomposition-based MOEAs [19], aiming to obtain the most suitable feasible solutions. Then, in [20], some researchers improved the existing constraint dominance principle based on information from objective functions. During the archiving process, feasible solutions are prioritized as the primary selection candidates. To further meet

the algorithm's requirements for solution feasibility, a strict constraint dominance principle was also designed.

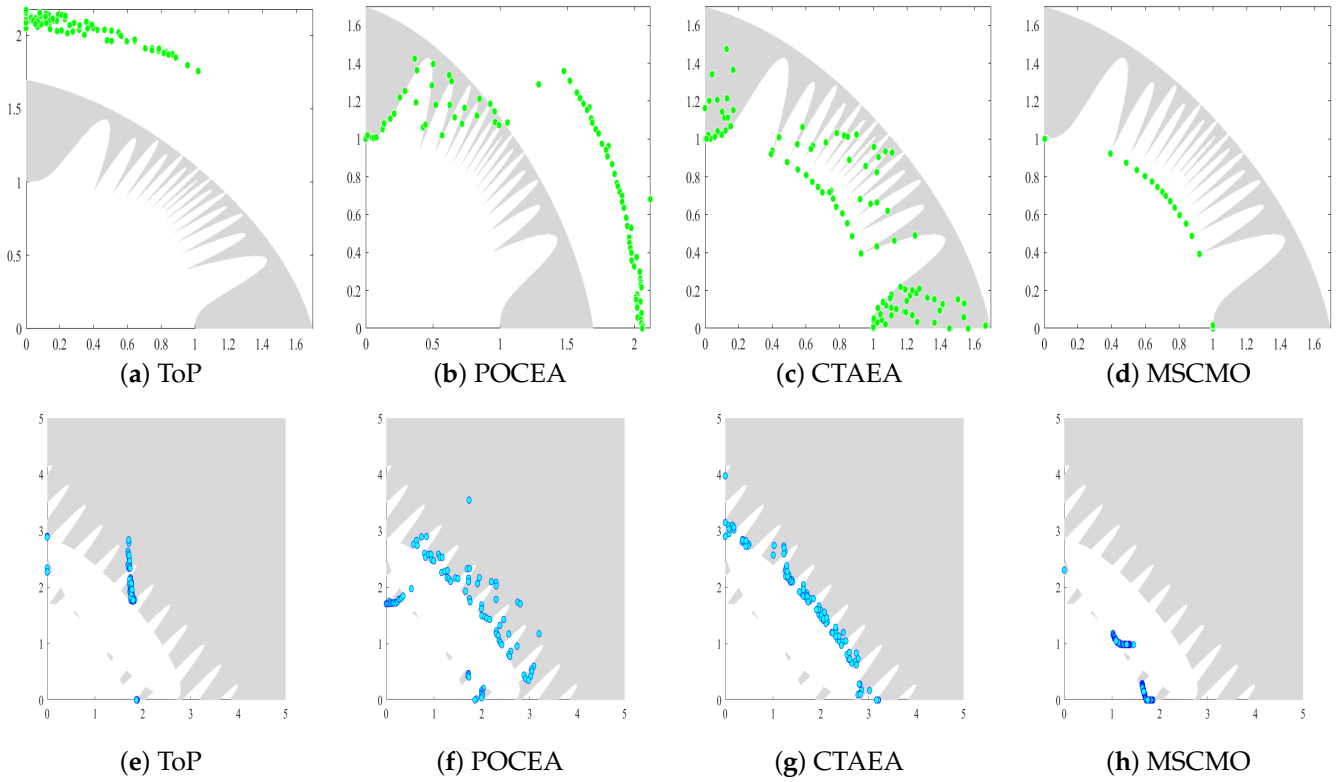
(2) Second category: Constraints and objectives have the same priority. To treat objectives and constraints equally, a three-matrix cooperative evolution framework was proposed in [21]. The three matrices represent objective values, constraint values, and their combination. Non-dominance ranks are established based on these matrices. In [22], rankings are separately conducted for objective values and constraint violation degrees. Solutions are then evaluated for non-dominance based on these two rankings to determine candidate solutions. Some researchers, to broaden the solution requirements, have modified certain objective functions [23] and incorporated these objective functions into the constraint combinations. This is used as a criterion to determine candidate solutions. In [24], feasible and infeasible weight vectors are set for objective values and constraints, respectively, to deepen the utilization of infeasible regions. The algorithm considers only objectives in archive population selection and uses the SDE distance as a criterion for determining candidate solutions.

(3) Third category: This category concerns maintaining a balance between objectives and constraints through multiple populations and multi-stage approaches. Wang et al. [25] proposed a three-stage adaptive trade-off model (ATM), where each stage is designed with different handling methods for objective functions and constraint violations. This approach expands the algorithm's ability to handle solutions and improves its feasibility. In the exploration of infeasible regions, Fan et al. [26] designed a push–pull search (PPS) framework, which separates objectives and constraints and considers them in phases. The push phase focuses solely on objectives, ignoring constraint limitations, while the pull phase simultaneously considers both objectives and constraints to maintain feasibility and ensure comprehensive logical validation of the algorithm. In ToP [27], the decomposition concept of CMOEA is embedded into a two-stage framework. In the first stage, the multi-objective problem is decomposed into single-objective problems. Building upon this, in the second stage, constraints are added to each objective, and CMOEA is used to handle them. The recently proposed CMOEA-MS [11] further enhances the satisfaction of objectives and constraints by adaptively adjusting them based on feedback from the proportion of feasible solutions. Based on such methods, some researchers have designed the dual-archive concept [9,13], which aims to separately consider objectives and constraints. One stage focuses on objectives, while the other focuses on constraints. Then, weak cooperation is conducted based on feedback from both archives to enhance the algorithm's balance between constraint satisfaction and objective optimization.

2.2. Motivations

In reviewing previous CMOEAs, we found that maintaining population diversity during population iteration makes it difficult for many algorithms to effectively handle CMOP benchmark problems. The main reason for this is that the population cannot traverse large and narrow infeasible regions, preventing it from obtaining the complete feasible region. To overcome these issues, researchers have enhanced the interaction capabilities between populations to gather more information about infeasible solutions. This significantly improves the search performance of the algorithm and prevents it from becoming trapped in local optima. To further validate our proposed theory, we selected two complex CMOPs (MW5 and LIRCMOP9) with large infeasible regions to illustrate the current shortcomings of CMOEAs. Through Figure 1, we can observe the constraint Pareto front (CPF) of four representative CMOEAs (i.e., ToP [27], POCEA [28], CTAEA [9], and MSCMO [29]) on MW5 and LIRCMOP9. The blue dots and green dots represent

the distribution of solutions obtained by the algorithm on the MW5 test problem and the LIRCMOP9 test problem, respectively. As shown in Figure 1a,d, both algorithms failed to find the true CPF. The main reason is the poor overall search performance of the algorithms, which prevents them from exploring the entire objective space. In contrast, as shown in Figure 1b,c,e,f,h, although all four algorithms found the CPF, they were unable to fully capture the CPF because the algorithms could not cross the narrow infeasible regions. For Figure 1d, all solutions of CTAEA lie on the CPF, but they are not evenly distributed across the CPF, mainly due to the inability to traverse the narrow and large infeasible regions.



(**a**) ToP (**b**) POCEA (**c**) CTAEA (**d**) MSCMO

(**e**) ToP (**f**) POCEA (**g**) CTAEA (**h**) MSCMO

Figure 1. Solution distribution of 4 CMOEAs on 2-objective MW5 and LIRCMOP9.

Based on the aforementioned theoretical knowledge, it is evident that fully utilizing information from infeasible solutions is an effective method for maintaining population diversity and obtaining a complete CPF. Building on this foundation, Qiao et al. [30] proposed a scalable high-dimensional constraint algorithm called IMTCMO. Based on a multi-population framework, the algorithm incorporates auxiliary tasks to enhance the interaction capabilities between populations. Auxiliary populations can promptly transfer useful information to the main population, enhancing its exploration capability of infeasible regions. This helps the main population to traverse infeasible areas and achieve a complete CPF. Although IMTCMO indirectly increases the interaction capabilities between populations and significantly enhances the algorithm's exploration of infeasible regions, it lacks effective methods for utilizing solution information. This leads to the transfer of most information about redundant solutions, which greatly wastes the algorithm's resources and exploration capacity. Tian et al. [31] designed a multi-population temporary archiving algorithm named TPCMaO. This algorithm not only enhances the interaction capabilities between populations but also incorporates an adaptive parameter for assessing solution constraints, which helps in selecting the most promising solutions. This greatly improves the overall performance of the algorithm. Although the algorithm is capable of traversing

large infeasible regions, it does not set reasonable criteria when using adaptive parameters to assess solution quality, resulting in the algorithm not obtaining a higher-quality CPF.

To address the challenges faced by the aforementioned algorithms, this paper proposes a constraint multi-objective evolutionary algorithm based on feedback tracking constraint relaxation, named CMOEA-FTR. This algorithm not only demonstrates high search performance when dealing with CMOPs of different characteristics but also maintains population diversity. To fully utilize information from infeasible solutions, the algorithm incorporates a strict secondary dominance principle strategy to ensure the algorithm's feasibility. To address the challenge of solution selection pressure, a temporary archive is designed. The archive is updated through the algorithm's iterations based on a new fitness ranking, significantly improving the algorithm's efficiency. Overall, CMOEA-FTR not only can traverse large infeasible regions but also maintains population diversity when handling CMOPs with different characteristics.

3. The Proposed CMOEA-FTR

In this section, not only is an overall description of the proposed CMOEA-FTP provided, but each innovative component is also analyzed and explained in detail. This serves to validate the unique competitiveness and superiority of CMOEA-FTP.

3.1. Framework of CMOEA-FTR

Algorithm 1 outlines the overall flowchart of CMOEA-FTR. First, the main population P_M generates a population of size N in the decision space. Then, the CV values of the solutions in P_M are calculated using Equation (3), and solutions with ing $CV == 0$ are stored in the archive population P_A to ensure the feasibility of the algorithm. Next, the maximum total constraint violation is set as the initial constraint relaxation boundary ω^0. Then, CMOEA-FTR formally enters the dual-phase iterative evolution process. To ensure fairness between the two phases, a is set to 0.5. As the iterations proceed, the constraint relaxation value ω^t is determined using Equation (9). With the continuous relaxation of the constraint boundary, many redundant solutions may appear. Therefore, the fitness of the solutions in P_M and P_A is calculated and ranked, and the redundant solutions in P_M and P_A are eliminated based on their rankings. The novel fitness evaluation introduces both diversity and convergence metrics for a comprehensive assessment. The mathematical definition of convergence is as follows:

$$R_x = \sum_{y \in \mathcal{C}, y \neq x} r_{(x,y)} \tag{4}$$

where $r_{(x,y)}$ represents the number of solutions that dominate x. The mathematical definition is as follows:

$$r_{(x,y)} = \begin{cases} 1, & \text{if } y \prec_{\mathbf{CDP}} x \\ 0, & \text{otherwise} \end{cases} \tag{5}$$

$y \prec_{\mathbf{CDP}} x$ represents the decision rule of the constraint dominance principle. The mathematical formula for the definition of diversity is as follows:

$$D(x) = \frac{1}{\sum_{i=1}^{k} d(x, \Omega_i) + 2} \tag{6}$$

where $d(x, \Omega_i)$ represents the k-nearest neighbor distance of solution x, which is used to differentiate the quality of diversity based on the crowding degree of the solutions.

The higher the crowding degree, the better the diversity, and vice versa. Considering both diversity and convergence, the definition of fitness is as follows:

$$fitness(x) = \sum_{y \in C, y \neq x} |R_x| + D_x \tag{7}$$

where R_x represents the convergence of solution x. When R_x is smaller, it means that fewer solutions dominate x, indicating that x is closer to the CPF, which signifies better convergence. Conversely, a larger R_x suggests poorer convergence. D_x represents the diversity of the solution x.

Then, an elite mating pool with an embedded balance factor is used to select high-quality parents M_1 from P_M and P_A, ensuring a balance between diversity and convergence of the algorithm. M_1 then generates offspring Q_1 through genetic operators. Finally, the combined population P_M, P_A , and Q_1 are updated and saved based on fitness rankings to form P_A. The combined population P_M, P_A, and Q_1 then generate a new population P_M through environmental selection according to SPEA2.

When the stage determination criteria are met, the algorithm proceeds to the second phase for iteration. Once the algorithm enters the second phase, the constraint relaxation is immediately halted. P_A and P_M use an empty initial population temp for solution exchange. The combined population P_M and P_A then select parents M_2 using an equal-probability elite mating pool selection mechanism to enhance the algorithm's feasibility and convergence. Subsequently, M_2 generates offspring Q_2 using DE operators. Finally, the combined population P_M, P_A, and Q_2 are updated and saved based on fitness rankings to form the final archive population P_A. The combined population P_M and Q_2 then generate the final population P_M through elite environmental selection. If the algorithm has not met the termination condition, the next iteration of the second phase is performed. To help readers better understand the two-phase transition and feedback tracking process of CMOEA-FTR, we have created a simplified flowchart of CMOEA-FTR, as shown in Figure 2.

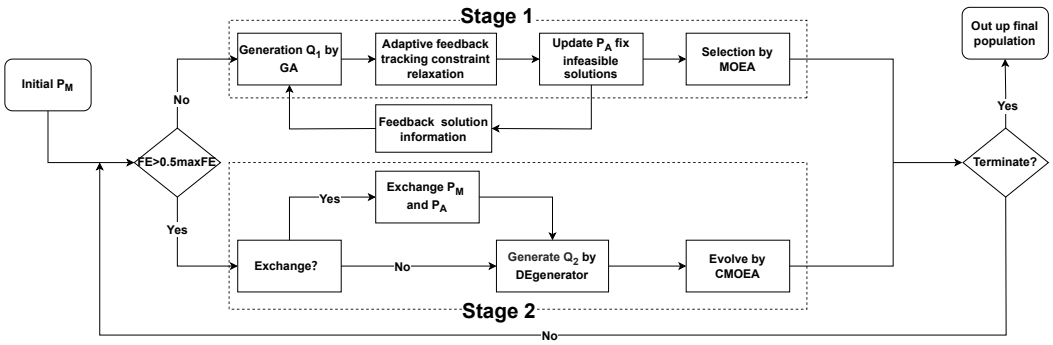


Figure 2. Framework flowchart of CMOEA-FTR.

CMOEAs are unable to find the global optimal solution when facing multi-objective optimization problems—they can only get arbitrarily close to the CPF. The main reason for this is that most multi-objective optimization problems are non-convex, and a single optimization algorithm cannot find the global optimum. Mathematical methods, when seeking the optimal solution, are often influenced by problem size, computational complexity, and multi-objective characteristics, making them impractical for real-world problems and unable to balance the conflicts between objectives and constraints. In contrast, by embedding heuristic methods (such as genetic algorithms and differential evolution) into the CMOEA-FTR framework, it is not only possible to find the best possible approximate solution within a reasonable time, but also effectively handle large-scale, complex multi-objective problems while meeting the practical demands of cost, efficiency, and loss.

Algorithm 1 Framework of CMOEA-FTR

Input: N (population size), P_A (Archive population), $temp$ (Null population), a (balance factor)
Output: P_M (final population)

$P_M \leftarrow$ Initialize the population (N);
Calculate the CV values of solutions in P_M using Formula (3);
$P_A \leftarrow P_M(|CV| == 0)$
$w^0 \leftarrow$ Find the maximum total constraint violation value of P_M;
while the terminal criterion is not fulfilled **do**
  if $FE \leq \alpha MaxFE$ **then**
    Calculate the ω^t for P_M using Formula (12);
    Calculate fitness of solutions in P_M,P_A using Formula (7);
    $M_1 \leftarrow$ MatingSelectionElite (P_M, P_A, N, a);
    $Q_1 \leftarrow$ Genetic operator (M_1);
    $P_A \leftarrow$ UpdateArchive ($P_M \cup Q_1$,P_A);
    $P_M \leftarrow$ Environmental selection in SPEA2 ($P_M \cup Q_1$, P_A);
  else
    if stage conver ==0 **then**
      $temp = P_M$
      $P_M = P_A$
      $P_A = temp$
      stage conver ==1
    end if
    $M_2 \leftarrow$ MatingSelectionElite (P_A, P_M, N, 0.5);
    $Q_2 \leftarrow$ DEgenerator2(M_2);
    $P_A \leftarrow$ UpdateArchive($P_M \cup Q_2$,P_A);
    $P_M \leftarrow$ Perform elite environment selection (P_M, Q_2);
  end if
end while

3.2. Adaptive Feedback Scaling Constraint Relaxation Mechanism

Based on the conventional constraint relaxation boundary learning, this paper designs a novel adaptive feedback scaling constraint relaxation mechanism, aimed at introducing more infeasible solutions. By tracking the feedback information from these infeasible solutions, the population's exploratory capability is enhanced, thereby obtaining a complete feasible region. As shown in Figure 2, the flowchart of the feedback tracking mechanism in the first stage generates the offspring Q_1, and then adaptively relaxes the constraints, incorporating more infeasible solutions as candidates for the archive. The archive modifies the solutions based on a new fitness ranking. As the iteration progresses, the archive feeds the modified solution information back to the previous generation of offspring. The offspring, based on the feedback information and the dominance principle, select the better offspring, continuing until the iteration ends. Finally, the MOEA without constraints is used to select the final population P_M of the first stage.

As shown in Figure 3a–c, the original constraint boundary relaxation mechanism eliminates [32] solutions close to the CPF (with smaller CV) to obtain more unknown regions and introduces solutions far from the CPF (with larger CV) into the population. Although this mechanism acquires more information about feasible solutions, it is very blind in the solution selection process and is likely to lose promising solutions close to the CPF. It also wastes computational resources and significantly reduces the overall performance of the algorithm. As shown in Figure 3a, before the relaxation mechanism starts, the infeasible solutions are sorted in descending order based on the CV obtained from Equation (3), and the lower-ranked solutions are eliminated. As shown in Figure 3b, the boundary begins to relax, allowing more solutions to be included. The solutions within the boundary are then sorted again in descending order of CV, and the lower-ranked solutions are eliminated. As shown in Figure 3c, after the constraint relaxation is completed,

a final descending order ranking of CV is performed. The top-ranked solutions are then added to the population.

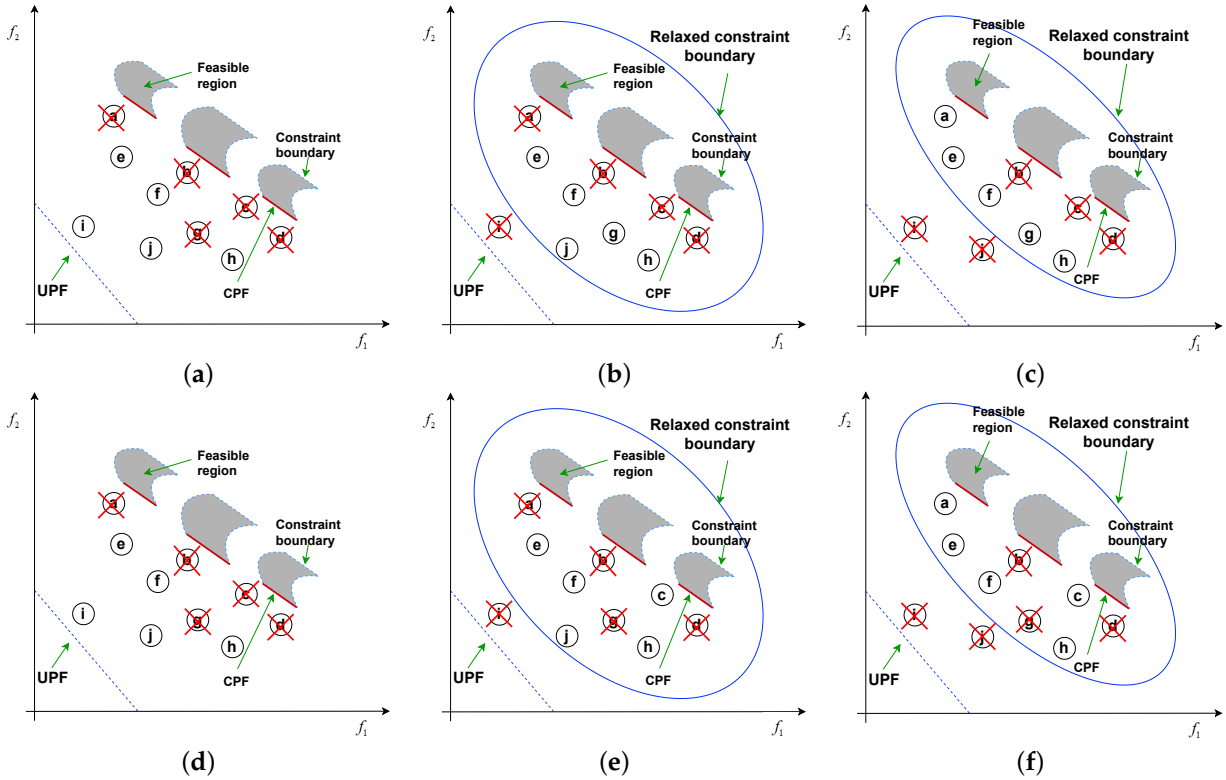


Figure 3. The entire process of adaptive feedback scaling constraint relaxation. Original constraint relaxation (**a**–**c**). Improved constraint relaxation (**d**–**f**).

Building on this, we improved the original solution selection process. As shown in Figure 3e,f, during the constraint boundary relaxation process, a new fitness ranking mechanism (Equation (7)) is applied to all solutions within the boundary, based on diversity ranking (Equation (6)) and convergence ranking (Equation (4)). The top N solutions are then selected. This approach not only obtains more information from infeasible solutions but also prevents the loss of promising solutions close to the CPF. In Figure 3e, after applying the fitness ranking mechanism to all infeasible solutions, the lower-ranked solutions are eliminated. As shown in Figure 3e, with the relaxation of the boundary, the fitness ranking within the boundary changes. The solutions are ranked again according to Equation (7), and the lower-ranked solutions are eliminated. For example, when solution j is added, solutions a and b are moved to lower ranks and eliminated, while solutions e, f, and c move up in rank and are retained. As shown in Figure 3f, after the constraint boundary relaxation is completed, all solutions within the boundary are ranked again. Although solution a is close to the CPF, it is retained due to its high rank.

In this paper, two adaptive metrics are added to the existing constraint relaxation mechanism. The constraint boundary values are continuously adjusted during the iterative evolution process based on the feedback metrics from the population solutions, maintaining the constraint values within a stable boundary. By tracking the newly added high-quality solutions, more feasible regions are obtained, further expanding the solution selection space. This approach not only allows for obtaining more solution information but also conserves

the algorithm's limited resources. The mathematical model for the current constraint relaxation mechanism [33] is as follows:

$$\begin{aligned} &\text{Minimize } F'(x) = (f_1(x), \cdots, f_m(x), CV(x)) \\ &\qquad g(x) \leq \omega^t \\ &\text{Subject to } \omega^t = \left(\omega_1^t, \cdots, \omega_q^t\right), t = 0, \cdots, T \\ &\qquad x \in \Omega \end{aligned} \tag{8}$$

In the above formula, ω^t is the boundary value for constraint relaxation. t represents the current iteration number of the algorithm. The introduced adaptive metrics are the average fitness β and the average violation ε, respectively. The specific calculation of β and ε is as follows:

$$\beta = \frac{1}{N}\sum_{i=1}^{N}(g_i(x) - Z_{min})a \tag{9}$$

Here, $g_i(x)$ represents the inequality constraint value value of the i-th solution, Z_{min} represents the smallest objective value of solution x, and a stands for scaling factor as shown in Equation (15).

$$\varepsilon = \frac{1}{N}\sum_{i=1}^{N}|CV_i(x) - CV_{max}| \tag{10}$$

In the above formula, $CV_i(x)$ represents the total constraint violation of the i-th solution, and CV_{max} is the largest total constraint violation associated with solution x.

The motivation for introducing the two metrics is as follows: (1) Throughout the entire iterative process, the size of the constraint boundary value is adaptively adjusted based on the feedback information β and ε from the population solutions. This not only increases the diversity of the population but also provides more information about the solutions, thereby enhancing the population's exploratory ability and preventing it from getting trapped in local optima. (2) The size of the constraint boundary value is adjusted adaptively based on β and ε. According to Formula (11), when β is large, β is selected. This results in the population introducing more solutions. By removing redundant solutions according to Formula (7), more solutions with smaller objective values will emerge, thereby reducing the average fitness. When ε is large, after the introduced solutions are filtered using Formula (7), the number of feasible solutions will increase compared to the original set. As a result, the average violation will begin to decrease accordingly.

Based on the derivation of the above theory, the derivation formula for ω^t is obtained as follows:

$$\omega = \max(\beta, \varepsilon) \tag{11}$$

$$\omega^t = \omega\left(1 - \frac{t}{T}\right)^{\frac{4-\ln|\omega|}{\ln(\lambda)}} \tag{12}$$

In the process of determining ω^t, λ represents the rate of change of the algorithm. Based on the proof from the equidistant experiments, we set it to 0.4 as the most suitable value.

In the original relaxation process, the focus was solely on increasing the number of infeasible solutions and enhancing diversity, which overlooked the quality of the solutions themselves, leading to a significant decline in convergence. To maintain a balance between diversity and convergence, this paper introduces an archive update mechanism that selects high-quality solutions to promote faster convergence to the optimal solution. Finally, by feeding the archive information back to the offspring, higher-quality solutions are generated, balancing diversity and convergence. Therefore, CMOEA-FTR not only

improves diversity and convergence but also balances their relationship through the feedback mechanism.

3.3. The Elite Mating Selection

Algorithm 2 [33] describes the process of selecting high-quality parents for the elite mating pool by tracking the optimal solutions from the first stage. The main population P_M and the archive population P_A are combined to generate U, and the number of feasible solutions N_f in P_M is calculated using Formula (3). If either N_F or the number of solutions in the archive population P_A is less than N, two solutions are randomly selected from the combined population U. By calculating the density values of these two solutions, the one with the smaller density is chosen for supplementation to enhance the algorithm's exploration ability. The specific formula for density is as follows:

$$Density(i) = \frac{1}{dis_i^l + 1} \tag{13}$$

$dis_i^l + 1$ represents the Euclidean distances from the first individual to its l nearest neighbors. The value of l is as follows:

$$l = \lfloor \sqrt{N} \rfloor + 1 \tag{14}$$

Conversely, if either N_f or the number of solutions in P_A is greater than N, P_M and P_A are filtered based on the balance factor to ensure the algorithm's diversity and convergence. The derivation formula for the balance factor a is as follows:

$$a = fr\left(1 - \cos\left((1 - \frac{t}{\mathrm{T}})\pi\right)\right) \tag{15}$$

fr represents the proportion of feasible solutions in a given iteration, t represents the current generation, and T represents the maximum number of generations.

When $rand < a$, two arbitrary solutions are selected from P_A. Since the constraint relaxation mechanism is mainly reflected in the main population P_M, solutions in P_A use the popular CDP method to select their dominant solutions as parents. If the two solutions do not dominate each other, the one with the smaller density is selected. The specific CDP rules are as follows:

$$\mathrm{x} \prec \mathrm{y} \Rightarrow \begin{cases} g(\mathrm{x}) < g(\mathrm{y}), & \text{if } f_{cv}(\mathrm{x}) = f_{cv}(\mathrm{y}) = 0 \\ f_{cv}(\mathrm{x}) < f_{cv}(\mathrm{y}), & \text{otherwise} \end{cases} \tag{16}$$

When $rand > a$, two arbitrary solutions are selected from P_M. Since P_M employs a constraint relaxation mechanism, we reduce the strictness of feasible solution determination on the original CDP [34], classifying some infeasible solutions as feasible. This allows the algorithm to obtain more information about solutions, enhancing its exploration ability in unknown areas and ensuring the population's diversity and convergence. If the two solutions exhibit mutual non-dominance, their density values are calculated, and the one with the smaller density is selected as the parent. The novel CDP is as follows:

$$\mathrm{x} \prec \mathrm{y} \Rightarrow \begin{cases} g(\mathrm{x}) < g(\mathrm{y}), & \text{if } f_{cv}(\mathrm{x}) \le \omega^t \\ & \text{and } f_{cv}(\mathrm{y}) \le \omega^t \\ & \text{or } f_{cv}(\mathrm{x}) = f_{cv}(\mathrm{y}) \\ f_{cv}(\mathrm{x}) < f_{cv}(\mathrm{y}), & \text{otherwise} \end{cases} \tag{17}$$

When the number of solutions in the final mating pool M_1 reaches N, all operations on the mating pool are terminated.

Algorithm 2 The elite mating selection

Input: P_M (main population), P_A (Archive population), N (population size)
Output: M_1 (mating pool)

$U \leftarrow P_M \cup P_A$;
$N_f \leftarrow$ Calculate the number of feasible solutions in P_M;
if $N_f < N$ or $|P_A| < N$ **then**
  Randomly select two solutions from U;
  Calculate the density of the two solutions using Formula (15);
  $M_1 \leftarrow$ Select the solution with the smaller density;
else
  if $rand < a$ **then**
    Randomly select two solutions (x_a and x_b) in P_A;
    Determine its dominance relationship using Formula (16);
    if $x_a \prec x_b$ **then**
      $M_1 \leftarrow x_a$;
    else if $x_b \prec x_a$ **then**
      $M_1 \leftarrow x_a$;
    else
      $M_1 \leftarrow$ Select the solution with lower density;
    end if
  else
    Randomly select two solutions (x_a and x_b) in P_M;
    Determine its dominance relationship using Formula (17);
    if $x_a \prec x_b$ **then**
      $M_1 \leftarrow x_a$;
    else if $x_b \prec x_a$ **then**
      $M_1 \leftarrow x_a$;
    else
      $M_1 \leftarrow$ Select the solution with lower density;
    end if
  end if
end if

3.4. ingUpdatedArchive

Algorithm 3 outlines the steps for updating the archive. When the number of solutions in P_A is less than N, the combined population (P_A, Q_2, and P_M) U is sorted in ascending order of CV. The solutions up to and including the Nth solution are selected as supplements. This adds more information about infeasible solutions, enhancing the algorithm's exploratory capability and increasing population diversity. Otherwise, the convergence R_x of the solutions in P_A is calculated using Equation (4), and the diversity D_x of the solutions in P_A is calculated using Equation (6). The larger the R_x, the weaker its dominance ability and the further it is from the CPF. The larger the D_x, the more uniform the distribution of solutions and the better the diversity. Therefore, R_x and D_x are fitted together as shown in the ninth column. The largest redundant solution F_x is continuously removed, keeping the archive with N solutions. Finally, the updated archive is saved and output.

Algorithm 3 UpdatedArchive

Input: N (population size), P_M (main population), Q (offspring population), P_A (Archive population)
Output: Updated*Archive*

$U \leftarrow P_M \cup P_A \cup Q$;
Add feasible solutions from P_M to P_A using Formula (3).
if $P_A \leq N$ **then**
  Calculate the CV values of solutions in U using Formula (3);
  Sort U in ascending order according to CV;
  $P_A \leftarrow$ Select the first N solutions;
else
  $R_x \leftarrow$ Calculate the convergence of the solutions in P_A using Formula (4);
  $D_x \leftarrow$ Calculate the diversity of the solutions in P_A using Formula (6);
  $F_x \leftarrow R_x + D_x$
  Updated*Archive* $\leftarrow$ Delete redundant solutions with maximum F_x;
end if
return Updated*Archive*

4. Experimental Studies

In this section, the setup and experiments for the research are first explained. Then, we describe the comparative experiment we conducted using seveb advanced CMEOAs and CMOEA-FTR on 44 CMOPs with different characteristics and 16 real-world application cases to validate the proposed theory. Finally, it is concluded that CMOEA-FTR is highly competitive.

4.1. Experimental Settings

This subsection explains all the settings involved. In the entire research process, the objective function, decision space, and constraints are represented by N, M, and D, respectively.

4.1.1. Test Problems

The settings of the 44 CMOPs, covering three benchmark test sets (MW, LIRCMOP, and ZXH_CF) and 16 real-world application cases (RWMOP), are as follows. Here, M represents the number of objectives and D represents the decision space. The detailed explanation is as follows:

(1) In MW1-14, all D values are set to 15. MW1-3, MW5-7, and MW9-13 have M set to two, while MW4, MW8, and MW14 are set to three objectives.
(2) In LIRCMOP1-14, D is set to 30. LIRCMOP1-12 hastwo objectives, while LIRCMOP13-14 has three objectives.
(3) In ZXH_CF1-16 and ZXH_CF1-12, three objectives are used with D set to 13. ZXH_CF13-16 has two objectives with D set to 12.
(4) RWMOP1-7, RWMOP9-10, RWMOP5-7, RWMOP12, and RWMOP14-16 have M set to two, while RWMOP8, RWMOP13, and RWMOP11 have three, three, and five objectives, respectively. As for D, it remains unchanged according to the original settings.

4.1.2. Compared Algorithms

In this paper, we use eight advanced CMOEAs as comparison experiment subjects (i.e., CTAEA [9], ToP [27], POCEA [28], TiGE2 [35], CMOEA_MS [11], CMOEMT [36], and TPCMaO [31]). The settings of the comparison algorithms follow their original papers without any modifications to ensure fairness. The specifics involved are as follows:

(1) Population size: The population size N for all algorithms is set to 100.
(2) Genetic operators: Some CMOEAs using GA operators refer to Simulated Binary Crossover (SBX) [37] and Polynomial Mutation (PM) [16] without any modifications.

(3) Terminal conditions: In this paper, the termination condition for all algorithms is set to MAXFE, which is 100,000. The algorithm stops running when the number of evaluations reaches 100,000.
(4) Performance indicator: This paper uses the Inverted Generational Distance (IGD) and Hypervolume (HV) metrics to evaluate the diversity and convergence of CMOEAs. A smaller IGD indicates better algorithm performance, while a larger IGD indicates worse performance. An increase in HV signifies improved algorithm performance, whereas a decrease in HV signifies poorer performance.
(5) Statistical test method: All experiments involved in this paper are conducted on the PlatEMO [38] platform. Each algorithm is run independently for 20 iterations on the platform, and the average and standard deviation are recorded. Statistical analysis is performed using the Wilcoxon rank-sum test at a significance level of 0.05. In the experiments, $+$, $-$, and $\approx$ denote better than, worse than, and similar to other CMOEAs, respectively. The gray-highlighted parts in the table represent the optimal values.

4.1.3. Device Support

The experiments were conducted using an i5 processor with an x64 architecture, running a Windows 10 or newer operating system, and MATLAB version R2021a or later. For optimal performance and accuracy, MATLAB should be installed on the C drive rather than on a mechanical hard drive.

4.2. Analysis of IGD and HV Data

From Tables 1 and 2, we can clearly see the IGD and HV statistical results of the eight CMOEAs on MW, LIRCMOP, and ZXH_CF. The MW test set includes many narrow feasible regions to test whether the algorithm falls into local optima and whether it can find a CPF that is infinitely close to the UPF under the trade-off between multiple objectives and constraints. For example, in Figure 1a–d, the CPF of the MW test problem is set to be extremely narrow, mainly to test whether the algorithm can search the entire feasible region. Algorithms with poor search capabilities find it difficult to identify the complete CPF, which not only affects the overall performance of the algorithm but also wastes its resources. In the MW1-14 test problems, CMOEA-FTR achieved 13 optimal results in terms of the IGD metric, with only TPCMaO achieving the best result in MW4. CMOEA-FTR achieved 11 optimal results in terms of the HV metric. Judging by the IGD and HV metrics of the eight algorithms, although CMOEA-FTR performs worse than its competitors on a few test problems, overall, CMOEA-FTR outperforms the other seven competitors across MW1-14. From the perspective of constraint types, in the nonlinear constrained MW1-3 test problems, CMOEA-FTR is able to handle them efficiently and achieve the best values. It also achieved the best value in the random objective MW8 test problem. In the MW9-13 test problems with non-convex constraints, CMOEA-FTR also handled them effectively and achieved the best performance, indirectly demonstrating the strong competitiveness of CMOEA-FTR.

In contrast, the LRCMOP test suite not only includes narrow feasible regions but also establishes some discontinuous feasible regions, posing a significant challenge to the search performance of the algorithms. For example, in Figure 1e–h's LIRCMOP9 test problem, the feasible region's CPF is not only set to be narrow, but there are also large infeasible regions between the discontinuous feasible areas. Many advanced algorithms struggle to overcome this challenge, resulting in their inability to find the complete CPF. The primary purpose of this setup is to test whether the algorithm can traverse large infeasible regions to find the complete feasible domain, thereby identifying the global optimal PF. In the LIRCMOP1-14 test problems, CMOEA-FTR achieved eight optimal results in terms of the IGD metric and nine optimal results in terms of the HV metric. Clearly, CMOEA-FTR

demonstrates strong competitiveness when dealing with discontinuous feasible regions. In the nonlinear constrained LIRCMOP1-4 test problems, CMOEA-FTR significantly outperforms the seven competitors. In the non-convex constrained LIRCMOP9 test problem, it also handles the problem effectively and achieves the best value. Regarding the random objective LIRCMOP13-14, CMOEA-FTR only performs worse than CMOEA_MS in the LIRCMOP13 test problem. Therefore, CMOEA-FTR is capable of effectively handling various types of constraints in the LIRCMOP test problems.

Table 1. Statistical outcomes (avg ± std) of IGD values for eight CMOEAs on MW, LIRCMOP, and ZXH_CF problems.

Problem	*M*	*D*	CTAEA	ToP	POCEA	TiGE2	CMOEA_MS	CMOEMT	TPCMaO	CMOEA-FTR
MW1	2	15	3.3830e-2 (3.48e-2) −	NaN (NaN)	1.3089e-2 (4.57e-3) −	5.2463e-2 (6.51e-2) −	4.2037e-2 (6.54e-2) −	9.0638e-2 (4.42e-2) −	4.5571e-3 (1.02e-2) −	1.6273e-3 (6.62e-6)
MW2	2	15	1.8133e-2 (7.89e-3) −	1.7940e-1 (1.48e-1) −	1.3531e-1 (1.04e-1) −	5.4455e-2 (3.51e-2) −	2.4023e-2 (8.46e-3) −	4.0501e-2 (2.85e-2) −	2.0150e-2 (7.41e-3) −	3.9112e-3 (4.37e-5)
MW3	2	15	1.2954e-2 (2.52e-3) −	2.2097e-1 (3.23e-1) −	2.7188e-2 (1.48e-2) −	5.1052e-2 (4.79e-2) −	1.3648e-2 (5.31e-3) −	1.6305e-2 (3.24e-3) −	1.0593e-2 (8.95e-4) −	5.1205e-3 (1.78e-4)
MW4	3	15	6.4495e-2 (2.06e-2) −	7.2571e-1 (0.00e+0) ≈	5.4908e-2 (3.34e-3) −	1.2132e-1 (6.19e-2) −	4.9339e-2 (7.63e-3) −	1.1079e-1 (2.35e-2) −	4.0617e-2 (5.91e-4) +	4.1997e-2 (4.90e-4)
MW5	2	15	1.4127e-2 (4.15e-3) −	7.5416e-1 (0.00e+0) ≈	7.6855e-2 (2.34e-2) −	4.7386e-2 (9.07e-3) −	6.9010e-2 (1.22e-1) −	7.7276e-2 (2.06e-2) −	1.3111e-3 (1.10e-3) −	4.7347e-4 (9.08e-5)
MW6	2	15	1.0959e-2 (6.47e-3) −	7.3029e-1 (3.51e-1) −	5.7904e-1 (3.67e-1) −	2.3935e-1 (3.09e-1) −	1.7844e-1 (2.16e-1) −	3.6539e-2 (1.27e-2) −	1.5386e-2 (6.84e-3) −	4.6368e-3 (6.65e-3)
MW7	2	15	6.7262e-3 (5.04e-4) −	5.7367e-2 (9.94e-2) −	5.2727e-2 (6.31e-2) −	3.1073e-2 (1.10e-2) −	3.1495e-2 (2.92e-2) −	1.5659e-2 (3.63e-3) −	9.5188e-3 (1.31e-3) −	5.1892e-3 (3.30e-4)
MW8	3	15	5.4905e-2 (3.09e-3) −	6.9878e-1 (4.11e-1) −	3.0482e-1 (2.45e-1) −	5.5415e-1 (2.77e-1) −	5.2374e-2 (1.45e-2) −	7.0693e-2 (2.33e-2) −	6.5512e-2 (2.81e-3) −	4.3044e-2 (6.03e-4)
MW9	2	15	8.7774e-3 (1.69e-3) −	8.5441e-1 (8.52e-2) −	1.0676e-1 (2.11e-1) −	9.8392e-2 (2.12e-1) −	2.0160e-1 (2.60e-1) −	9.5902e-2 (2.11e-1) −	9.1794e-3 (1.72e-2) −	4.8779e-3 (3.00e-4)
MW10	2	15	2.6026e-2 (1.65e-2) −	NaN (NaN)	2.9326e-1 (1.81e-1) −	7.7929e-2 (5.48e-2) −	3.6383e-2 (1.90e-2) −	8.3408e-2 (5.89e-2) −	2.7612e-2 (1.68e-2) −	3.6954e-3 (1.40e-3)
MW11	2	15	2.0545e-2 (7.72e-3) −	5.2819e-1 (2.69e-1) −	6.3878e-2 (7.87e-2) −	3.7307e-2 (8.00e-3) −	1.4053e-2 (1.01e-2) −	1.8706e-2 (4.97e-3) −	4.2372e-2 (1.96e-2) −	6.1095e-3 (1.61e-4)
MW12	2	15	6.1014e-2 (1.82e-1) −	8.3690e-1 (0.00e+0) ≈	4.7754e-2 (1.01e-1) −	1.2301e-1 (2.26e-1) −	1.5524e-1 (2.82e-1) −	2.6368e-2 (1.05e-2) −	6.4998e-3 (2.63e-3) −	4.7527e-3 (8.47e-5)
MW13	2	15	6.3400e-2 (3.47e-2) −	1.0845e+0 (7.97e-1) −	4.7870e-1 (3.54e-1) −	4.5309e-1 (1.69e-1) −	5.0814e-1 (4.96e-1) −	1.0459e-1 (3.46e-2) −	5.1748e-2 (2.61e-2) −	1.2653e-2 (6.04e-3)
MW14	3	15	4.9614e-1 (3.99e-1) −	8.5539e-1 (8.65e-1) −	5.8826e-1 (5.27e-1) −	1.8182e-1 (3.86e-2) −	3.2031e-1 (1.88e-1) −	7.1254e-1 (1.98e-1) −	1.0211e-1 (6.97e-3) ≈	9.7846e-2 (1.69e-3)
ing+/ − / ≈			0/14/0	0/9/3	0/14/0	0/14/0	0/14/0	0/14/0	1/12/1	
Problem	*M*	*D*	CTAEA	ToP	POCEA	TiGE2	CMOEA_MS	CMOEMT	TPCMaO	CMOEA-FTR
LIRCMOP1	2	30	3.0813e-1 (9.45e-2) −	3.2853e-1 (2.16e-2) −	1.7640e-1 (1.36e-1) ≈	2.0840e-1 (1.37e-2) −	3.2481e-1 (4.71e-2) −	3.3986e-1 (1.69e-2) −	1.8831e-1 (4.79e-2) −	1.0630e-1 (4.86e-2)
LIRCMOP2	2	30	2.4246e-1 (9.34e-2) −	2.8906e-1 (2.18e-2) −	1.5439e-1 (1.02e-1) −	1.9456e-1 (1.79e-2) −	2.7883e-1 (4.45e-2) −	2.7467e-1 (3.39e-2) −	1.8150e-1 (3.88e-2) −	4.5037e-2 (1.45e-2)
LIRCMOP3	2	30	3.4241e-1 (1.64e-1) −	3.4399e-1 (1.64e-2) −	2.0752e-1 (9.07e-2) −	2.1517e-1 (1.30e-2) −	3.2129e-1 (4.27e-2) −	2.9253e-1 (4.21e-2) −	1.9635e-1 (4.48e-2) −	1.0499e-1 (4.53e-2)
LIRCMOP4	2	30	2.9330e-1 (5.13e-2) −	3.2278e-1 (1.21e-2) −	2.3693e-1 (9.22e-2) −	2.1541e-1 (2.53e-2) −	2.7799e-1 (4.96e-2) −	2.8009e-1 (3.38e-2) −	1.8657e-1 (2.79e-2) −	9.0362e-2 (4.71e-2)
LIRCMOP5	2	30	1.2229e+0 (2.19e-1) −	1.1161e+0 (2.81e-1) ≈	1.2393e+0 (9.41e-1) −	9.5812e-1 (4.11e-1) ≈	3.7233e-1 (2.04e-1) +	1.3044e+0 (1.84e-1) −	2.6072e-1 (5.97e-2) +	9.7858e-1 (4.79e-1)
LIRCMOP6	2	30	1.4359e+0 (3.20e-1) −	1.3467e+0 (4.70e-4) −	1.0393e+0 (6.30e-1) ≈	9.6675e-1 (4.14e-1) ≈	5.0159e-1 (3.69e-1) +	1.3602e+0 (1.47e-2) −	2.4780e-1 (8.56e-2) +	1.1407e+0 (4.29e-1)
LIRCMOP7	2	30	8.2863e-1 (7.43e-1) −	1.3804e+0 (6.23e-1) −	1.2660e+0 (1.05e+0) −	3.2249e-1 (1.50e-1) −	1.3986e-1 (3.98e-2) −	1.0872e+0 (6.90e-1) −	9.2170e-2 (2.42e-2) ≈	9.0501e-2 (4.13e-2)
LIRCMOP8	2	30	1.3794e+0 (7.07e-1) −	1.5448e+0 (4.26e-1) −	1.1036e+0 (1.04e+0) −	5.1108e-1 (3.28e-1) −	1.9733e-1 (3.83e-2) −	1.3836e+0 (5.53e-1) −	1.3850e-1 (4.31e-2) −	7.9180e-2 (6.86e-2)
LIRCMOP9	2	30	8.1715e-1 (2.97e-1) −	5.9781e-1 (1.38e-1) −	9.0584e-1 (3.05e-1) −	7.2148e-1 (9.51e-2) −	6.9448e-1 (1.45e-1) −	1.0183e+0 (1.42e-1) −	5.1332e-1 (1.20e-1) −	4.1445e-1 (1.11e-1)
LIRCMOP10	2	30	7.2617e-1 (4.02e-1) −	4.2407e-1 (5.83e-2) −	8.4783e-1 (3.40e-1) −	8.5507e-1 (1.84e-1) −	4.7126e-1 (1.46e-1) −	1.0074e+0 (9.14e-2) −	2.0409e-1 (6.08e-2) ≈	2.2031e-1 (1.30e-1)
LIRCMOP11	2	30	6.2374e-1 (4.03e-1) −	4.7327e-1 (1.14e-1) −	7.8143e-1 (3.27e-1) −	7.9533e-1 (2.53e-1) −	3.5132e-1 (1.61e-1) −	9.3467e-1 (1.50e-1) −	8.7599e-2 (5.88e-2) ≈	1.3110e-1 (1.35e-1)
LIRCMOP12	2	30	6.5436e-1 (4.89e-1) −	3.1726e-1 (7.74e-2) −	7.1277e-1 (3.84e-1) −	4.5723e-1 (9.00e-2) −	3.9776e-1 (1.40e-1) −	8.7013e-1 (2.83e-1) −	2.1075e-1 (8.92e-2) ≈	2.0685e-1 (9.93e-2)
LIRCMOP13	3	30	7.2146e-1 (6.26e-1) −	1.3129e+0 (9.95e-2) −	7.9913e-1 (6.11e-1) −	1.2939e+0 (3.17e-1) −	9.4959e-2 (2.80e-3) +	2.7971e-1 (2.22e-2) −	1.2963e-1 (4.03e-3) −	1.0359e-1 (1.94e-3)
LIRCMOP14	3	30	1.1114e-1 (1.37e-3) −	1.3028e+0 (6.03e-3) −	9.6798e-1 (5.67e-1) −	1.3102e+0 (2.15e-1) −	9.7374e-2 (2.81e-3) ≈	2.4478e-1 (1.47e-2) −	1.4625e-1 (5.05e-3) −	9.8193e-2 (7.79e-4)
+/ − / ≈			0/14/0	0/13/1	0/12/2	0/12/2	3/10/1	0/14/0	2/8/4	
Problem	*M*	*D*	CTAEA	ToP	POCEA	TiGE2	CMOEA_MS	CMOEMT	TPCMaO	CMOEA-FTR
ZXH_CF1	3	13	4.8756e-2 (1.50e-3) +	9.7660e-2 (1.56e-2) −	5.2941e-2 (1.79e-2) +	1.2369e-1 (1.36e-2) −	4.9308e-2 (1.25e-3) +	5.2649e-2 (1.43e-3) ≈	4.1163e-2 (3.68e-4) +	5.3032e-2 (1.31e-3)
ZXH_CF2	3	13	9.6657e-2 (8.65e-2) −	3.1536e-1 (1.70e-1) −	1.5956e-1 (8.97e-2) −	2.6961e-1 (2.47e-1) −	1.4038e-1 (2.63e-1) −	6.4230e-2 (1.64e-3) −	8.8844e-2 (4.04e-2) −	5.8684e-2 (8.09e-4)
ZXH_CF3	3	13	7.5642e-2 (2.67e-3) ≈	2.2845e-1 (5.99e-2) −	1.8446e-1 (3.52e-2) −	1.2760e-1 (1.07e-2) −	8.2462e-2 (3.86e-3) −	6.7928e-2 (1.69e-3) +	9.6553e-2 (7.91e-3) −	7.6190e-2 (2.37e-3)
ZXH_CF4	3	13	1.1208e-1 (6.64e-2) ≈	1.2052e+0 (2.55e-1) −	7.1163e-1 (4.22e-1) −	3.0388e-1 (2.33e-1) −	2.5642e-1 (3.04e-1) −	1.1381e-1 (7.27e-2) ≈	1.1693e-1 (5.22e-2) ≈	1.1983e-1 (6.93e-2)
ZXH_CF5	3	13	5.7842e-2 (3.25e-2) −	1.1952e-1 (5.06e-2) −	8.5074e-2 (1.55e-2) −	1.9909e-1 (3.17e-1) −	1.5666e-1 (3.91e-1) −	4.5666e-2 (1.87e-2) −	3.1288e-2 (1.44e-3) +	3.4224e-2 (1.01e-3)
ZXH_CF6	3	13	3.6313e-2 (1.60e-3) −	5.6768e-2 (7.17e-3) −	7.0337e-2 (1.44e-2) −	5.9488e-2 (3.42e-3) −	3.3786e-2 (9.61e-4) −	3.5051e-2 (6.08e-4) −	3.8577e-2 (2.19e-3) −	3.1794e-2 (8.94e-4)
ZXH_CF7	3	13	9.3481e-2 (6.01e-2) ≈	5.5079e-1 (2.46e-1) −	6.2444e-1 (4.54e-1) −	2.2175e-1 (2.13e-1) ≈	2.6985e-1 (2.08e-1) −	7.5257e-2 (6.45e-2) ≈	7.5262e-2 (5.42e-2) +	1.4975e-1 (2.12e-1)
ZXH_CF8	3	13	5.6277e-2 (5.62e-3) −	2.4528e-1 (3.62e-1) −	1.3624e-1 (2.52e-2) −	7.3875e-2 (6.42e-3) −	1.5169e-1 (2.76e-2) −	4.0841e-2 (1.95e-3) −	3.0875e-2 (5.41e-4) +	3.4741e-2 (9.89e-4)
ZXH_CF9	3	13	6.5038e-2 (1.40e-2) −	5.1171e-1 (1.21e-1) −	3.8132e-1 (1.95e-1) −	1.0999e-1 (1.97e-2) −	1.4279e-1 (1.06e-1) −	3.0373e-2 (9.33e-4) −	3.7565e-2 (2.71e-3) −	2.6920e-2 (5.70e-4)
ZXH_CF10	3	13	1.2220e-1 (8.04e-2) −	1.1566e+0 (4.25e-1) −	1.1922e+0 (4.89e-1) −	1.6023e-1 (4.26e-2) −	3.6530e-1 (3.20e-1) −	9.2758e-2 (6.50e-2) −	7.6029e-2 (5.80e-2) −	5.8406e-2 (5.26e-2)
ZXH_CF11	3	13	3.5532e-2 (9.70e-4) −	5.1396e-1 (2.09e-1) −	6.9402e-2 (6.93e-3) −	1.8884e-1 (3.04e-2) −	2.9348e-2 (3.45e-4) −	3.0692e-2 (5.31e-4) −	4.0982e-2 (1.63e-3) −	2.8005e-2 (3.13e-4)
ZXH_CF12	3	13	7.5879e-2 (1.50e-1) −	4.8357e-1 (1.01e-1) −	1.1436e-1 (7.59e-2) −	2.4806e-1 (2.31e-1) −	1.0819e-1 (2.19e-1) −	2.9167e-2 (1.76e-3) −	3.4888e-2 (4.21e-2) −	2.3511e-2 (4.25e-4)
ZXH_CF13	2	12	7.4464e-2 (1.04e-1) −	9.5274e-1 (3.91e-1) −	7.8015e-1 (5.50e-1) −	1.2942e-1 (8.57e-2) −	3.2273e-1 (2.31e-1) −	9.4611e-2 (1.43e-1) −	9.4531e-2 (1.36e-1) −	5.7117e-2 (1.38e-1)
ZXH_CF14	2	12	2.8541e-3 (1.22e-4) −	1.4504e-1 (2.09e-1) −	1.6415e-2 (2.17e-3) −	3.5773e-2 (5.30e-3) −	2.5264e-3 (5.04e-5) −	3.3834e-3 (2.07e-4) −	2.3990e-3 (3.76e-5) −	2.3677e-3 (3.66e-5)
ZXH_CF15	2	12	5.6692e-3 (7.02e-4) −	1.8225e-1 (2.06e-1) −	3.5310e-2 (2.33e-2) −	7.1716e-2 (8.93e-2) −	2.6988e-2 (5.14e-2) −	2.0192e-2 (7.58e-2) −	8.9691e-3 (3.03e-3) −	2.8015e-3 (4.99e-5)
ZXH_CF16	2	12	1.4255e-2 (5.13e-3) −	2.7397e-2 (4.87e-2) −	1.5499e-2 (1.44e-3) −	2.9742e-2 (7.27e-3) −	8.3846e-2 (5.56e-2) −	2.6346e-3 (4.08e-5) −	9.4280e-3 (2.04e-3) −	2.5935e-3 (2.72e-5)
+/ − / ≈			1/12/3	0/16/0	1/15/0	0/15/1	1/15/0	1/12/3	4/11/1	
+/ − / ≈			1/40/3	0/38/4	1/41/2	0/41/3	4/39/1	1/40/3	7/31/6	

In addition to the MW and LIRCMOP test sets, this paper also references the highly extensible ZXH_CF test suite, where the objectives and decision variables are arbitrary. With the increase in objectives, it becomes extremely challenging to maintain a balance between objectives and constraints, which can easily lead to the algorithm being in a deadlock or failing to find feasible solutions. From the analysis of IGD in Table 1 and HV in Table 2, although CMOEA-FTR does not perform ideally on a few test problems, it generally outperforms other competitive algorithms across the ZXH_CF1-16 test problems. In the random objective ZXH_CF2 and ZXH_CF10 constrained test problems, CMOEA-FTR achieved the best performance. When faced with the nonlinear constraints in ZXH_CF13-16,

it outperformed the competitors, further demonstrating that CMOEA-FTR can effectively handle both nonlinear and random objective constraint types.

Table 2. Statistical outcomes (avg ± std) of HV values for eight CMOEAs on MW, LIRCMOP, and ZXH_CF problems.

Problem	*M*	*D*	CTAEA	ToP	POCEA	TiGE2	CMOEA_MS	CMOEMT	TPCMaO	CMOEA-FTR
MW1	2	15	4.4028e-1 (5.14e-2) −	NaN (NaN)	4.6778e-1 (8.81e-3) −	4.3091e-1 (5.71e-2) −	4.4701e-1 (5.90e-2) ≈	3.7795e-1 (3.83e-2) −	4.8514e-1 (1.21e-2) −	4.8996e-1 (4.68e-5)
MW2	2	15	5.5749e-1 (1.36e-2) −	3.7181e-1 (1.54e-1) −	4.0848e-1 (1.04e-1) −	5.1177e-1 (3.26e-2) −	5.4790e-1 (1.25e-2) −	5.2371e-1 (3.92e-2) −	5.5413e-1 (1.21e-2) −	5.8209e-1 (6.78e-5)
MW3	2	15	5.3036e-1 (5.69e-3) −	3.8019e-1 (1.79e-1) −	5.1197e-1 (2.20e-2) −	5.0679e-1 (3.05e-2) −	5.3372e-1 (6.42e-3) −	5.2490e-1 (6.74e-3) −	5.4470e-1 (5.86e-4) +	5.4390e-1 (2.97e-4)
MW4	3	15	8.0781e-1 (3.59e-2) −	1.1720e-1 (0.00e+0) ≈	8.2053e-1 (4.97e-3) −	7.5360e-1 (5.62e-2) −	8.2816e-1 (1.25e-2) −	7.4032e-1 (3.39e-2) −	8.3460e-1 (2.69e-3) −	8.3943e-1 (7.34e-4)
MW5	2	15	3.1575e-1 (3.06e-3) −	5.6763e-2 (0.00e+0) ≈	2.5604e-1 (2.97e-2) −	2.9680e-1 (5.95e-3) −	2.9085e-1 (3.74e-2) −	2.3863e-1 (2.70e-2) −	3.2398e-1 (4.55e-4) −	3.2440e-1 (6.63e-5)
MW6	2	15	3.1273e-1 (9.65e-3) −	7.1210e-2 (5.91e-2) −	9.8677e-2 (9.92e-2) −	2.2186e-1 (7.25e-2) −	2.5440e-1 (6.20e-2) −	2.7929e-1 (1.85e-2) −	3.1063e-1 (1.05e-2) −	3.2569e-1 (9.68e-3)
MW7	2	15	4.0939e-1 (6.45e-4) −	3.7013e-1 (3.75e-2) −	3.7044e-1 (3.95e-2) −	3.9406e-1 (3.86e-3) −	3.9918e-1 (2.22e-2) −	3.9896e-1 (4.10e-3) −	4.1176e-1 (5.17e-4) +	4.1109e-1 (6.60e-4)
MW8	3	15	5.1979e-1 (1.35e-2) −	1.2738e-1 (1.54e-1) −	2.8547e-1 (1.49e-1) −	2.0847e-1 (1.47e-1) −	5.2514e-1 (1.37e-2) −	4.7820e-1 (4.53e-2) −	5.3521e-1 (8.93e-3) −	5.5056e-1 (2.26e-3)
MW9	2	15	3.9136e-1 (4.57e-3) −	0.0000e+0 (0.00e+0) −	3.1255e-1 (1.05e-1) −	3.2957e-1 (1.13e-1) −	2.5257e-1 (1.48e-1) −	3.2620e-1 (7.81e-2) −	3.9370e-1 (1.72e-2) −	3.9567e-1 (1.97e-3)
MW10	2	15	4.2774e-1 (1.64e-2) −	NaN (NaN)	2.6992e-1 (8.49e-2) −	3.8532e-1 (3.36e-2) −	4.1888e-1 (1.66e-2) −	3.8526e-1 (3.58e-2) −	4.2583e-1 (1.51e-2) −	4.5418e-1 (2.69e-3)
MW11	2	15	4.3958e-1 (3.89e-3) −	3.0696e-1 (5.99e-2) −	4.2041e-1 (2.57e-2) −	4.3233e-1 (3.57e-3) −	4.4094e-1 (6.73e-3) −	4.4071e-1 (1.88e-3) −	4.3265e-1 (6.20e-3) −	4.4751e-1 (2.46e-4)
MW12	2	15	5.5480e-1 (1.32e-1) −	0.0000e+0 (0.00e+0) ≈	5.6168e-1 (8.68e-2) −	4.9722e-1 (1.90e-1) −	4.8489e-1 (2.14e-1) −	5.7818e-1 (1.60e-2) −	6.0333e-1 (2.04e-3) −	6.0470e-1 (3.17e-4)
MW13	2	15	4.5178e-1 (1.60e-2) −	1.6784e-1 (1.39e-1) −	2.5860e-1 (1.24e-1) −	3.2082e-1 (5.20e-2) −	3.3448e-1 (1.18e-1) −	4.3310e-1 (1.60e-2) −	4.5581e-1 (1.15e-2) −	4.7537e-1 (4.41e-3)
MW14	3	15	2.8965e-1 (1.83e-1) −	2.4175e-1 (1.88e-1) −	2.9586e-1 (1.68e-1) −	4.3891e-1 (1.65e-2) −	3.9108e-1 (8.24e-2) −	2.2506e-1 (7.75e-2) −	4.7518e-1 (1.71e-3) +	4.7047e-1 (1.20e-3)
ing+/ − / ≈			0/14/0	0/9/3	0/14/0	0/14/0	0/13/1	0/14/0	3/11/0	
Problem	*M*	*D*	CTAEA	ToP	POCEA	TiGE2	CMOEA_MS	CMOEMT	TPCMaO	CMOEA-FTR
LIRCMOP1	2	30	1.1153e-1 (2.82e-2) −	1.0174e-1 (9.76e-3) −	1.5953e-1 (5.44e-2) ≈	1.4146e-1 (6.14e-3) −	1.0830e-1 (1.23e-2) −	1.0091e-1 (4.59e-3) −	1.5025e-1 (2.06e-2) −	1.8086e-1 (2.26e-2)
LIRCMOP2	2	30	2.4258e-1 (5.15e-2) −	2.1439e-1 (1.74e-2) −	2.8226e-1 (5.06e-2) −	2.6515e-1 (8.62e-3) −	2.2503e-1 (2.03e-2) −	2.1985e-1 (1.55e-2) −	2.7118e-1 (1.76e-2) −	3.3189e-1 (1.16e-2)
LIRCMOP3	2	30	9.9568e-2 (2.44e-2) −	9.3085e-2 (5.54e-3) −	1.3158e-1 (2.68e-2) −	1.2988e-1 (6.94e-3) −	9.8505e-2 (1.27e-2) −	1.0345e-1 (1.17e-2) −	1.3697e-1 (1.28e-2) −	1.6233e-1 (1.35e-2)
LIRCMOP4	2	30	1.9572e-1 (2.13e-2) −	1.7739e-1 (1.21e-2) −	2.1458e-1 (4.01e-2) −	2.2270e-1 (1.17e-2) −	1.9938e-1 (2.30e-2) −	1.9454e-1 (1.38e-2) −	2.4001e-1 (1.41e-2) −	2.7823e-1 (1.70e-2)
LIRCMOP5	2	30	7.1968e-3 (3.22e-2) ≈	2.0299e-2 (6.39e-2) ≈	7.2046e-2 (1.16e-1) ≈	4.3036e-2 (6.80e-2) ≈	1.3863e-1 (4.05e-2) +	0.0000e+0 (0.00e+0) −	1.7028e-1 (2.32e-2) +	5.5141e-2 (1.13e-1)
LIRCMOP6	2	30	0.0000e+0 (0.00e+0) −	0.0000e+0 (0.00e+0) −	4.5566e-2 (5.91e-2) ≈	3.8927e-2 (4.08e-2) ≈	8.7316e-2 (3.86e-2) +	0.0000e+0 (0.00e+0) −	1.2842e-1 (1.46e-2) +	2.4284e-2 (5.38e-2)
LIRCMOP7	2	30	1.3077e-1 (1.14e-1) −	4.8767e-2 (1.01e-1) −	9.2152e-2 (1.16e-1) −	1.9985e-1 (2.55e-2) −	2.4346e-1 (1.15e-2) −	8.6706e-2 (1.00e-1) −	2.5829e-1 (7.43e-3) ≈	2.5867e-1 (1.50e-2)
LIRCMOP8	2	30	5.8184e-2 (9.46e-2) −	1.9875e-2 (6.15e-2) −	1.1464e-1 (1.07e-1) −	1.6923e-1 (5.11e-2) −	2.3102e-1 (7.74e-3) −	4.2404e-2 (7.75e-2) −	2.4695e-1 (1.02e-2) −	2.6591e-1 (2.25e-2)
LIRCMOP9	2	30	1.9810e-1 (1.38e-1) −	2.8476e-1 (8.05e-2) −	1.8196e-1 (1.10e-1) −	2.3237e-1 (7.89e-2) −	2.6528e-1 (5.93e-2) −	1.1293e-1 (6.34e-2) −	3.5668e-1 (5.50e-2) −	4.1724e-1 (6.10e-2)
LIRCMOP10	2	30	2.8484e-1 (2.46e-1) −	4.7631e-1 (6.28e-2) −	1.8828e-1 (1.65e-1) −	1.4833e-1 (4.61e-2) −	4.2822e-1 (1.28e-1) −	7.3399e-2 (2.80e-2) −	5.9071e-1 (3.71e-2) ≈	5.9359e-1 (7.10e-2)
LIRCMOP11	2	30	3.7493e-1 (2.26e-1) −	3.7436e-1 (8.42e-2) −	2.6700e-1 (1.47e-1) −	2.1275e-1 (9.66e-2) −	4.6917e-1 (1.14e-1) −	1.7346e-1 (7.21e-2) −	6.5200e-1 (3.60e-2) ≈	6.1977e-1 (8.29e-2)
LIRCMOP12	2	30	3.3161e-1 (1.95e-1) −	4.6118e-1 (4.01e-2) −	3.3562e-1 (1.20e-1) −	3.8103e-1 (5.36e-2) −	4.3360e-1 (5.43e-2) −	2.2078e-1 (1.02e-1) −	5.2043e-1 (4.14e-2) ≈	5.2047e-1 (4.97e-2)
LIRCMOP13	3	30	2.7248e-1 (2.80e-1) ≈	5.3778e-3 (1.68e-2) −	2.3106e-1 (2.54e-1) −	3.5692e-2 (1.17e-1) −	5.5430e-1 (2.08e-3) +	3.6032e-1 (1.87e-2) −	5.6108e-1 (9.74e-4) +	5.3360e-1 (2.45e-3)
LIRCMOP14	3	30	5.4616e-1 (9.14e-4) −	2.5125e-4 (2.75e-4) −	1.5822e-1 (2.43e-1) −	1.5500e-2 (6.90e-2) −	5.5415e-1 (1.90e-3) +	4.0060e-1 (1.50e-2) −	5.4987e-1 (1.81e-3) ≈	5.4984e-1 (1.04e-3)
+/ − / ≈			0/12/2	0/13/1	0/11/3	0/12/2	4/10/0	0/14/0	3/6/5	
Problem	*M*	*D*	CTAEA	ToP	POCEA	TiGE2	CMOEA_MS	CMOEMT	TPCMaO	CMOEA-FTR
ZXH_CF1	3	13	8.3464e-1 (1.25e-3) +	7.6055e-1 (2.29e-2) −	8.0689e-1 (5.10e-2) −	7.5475e-1 (1.62e-2) −	8.2610e-1 (2.35e-3) +	8.2047e-1 (1.95e-3) −	8.3666e-1 (9.37e-4) +	8.2317e-1 (1.62e-3)
ZXH_CF2	3	13	4.9353e-1 (1.25e-1) −	2.3984e-1 (1.04e-1) −	4.0154e-1 (8.37e-2) −	3.9404e-1 (1.45e-1) −	4.8976e-1 (1.68e-1) −	5.2960e-1 (3.51e-3) −	5.3412e-1 (7.69e-2) −	5.4499e-1 (1.52e-3)
ZXH_CF3	3	13	5.1163e-1 (2.57e-3) +	2.5602e-1 (5.77e-2) −	4.2994e-1 (1.99e-2) −	4.4603e-1 (1.25e-2) −	5.0770e-1 (2.85e-3) +	4.9615e-1 (3.61e-3) +	5.2871e-1 (1.74e-3) +	4.7826e-1 (5.26e-3)
ZXH_CF4	3	13	3.4425e-1 (9.58e-2) +	0.0000e+0 (0.00e+0) −	5.8954e-2 (1.29e-1) −	1.7839e-1 (1.38e-1) −	2.5523e-1 (1.73e-1) ≈	3.2821e-1 (9.97e-2) ≈	3.5332e-1 (9.02e-2) +	3.1634e-1 (9.45e-2)
ZXH_CF5	3	13	2.7618e-1 (4.36e-2) −	1.9029e-1 (4.81e-2) −	2.4109e-1 (1.24e-2) −	2.0341e-1 (9.31e-2) −	2.7456e-1 (9.39e-2) −	2.8224e-1 (2.58e-2) −	3.0832e-1 (3.56e-3) +	3.0152e-1 (1.65e-3)
ZXH_CF6	3	13	2.2440e-1 (1.01e-3) +	1.9209e-1 (8.92e-3) −	1.8694e-1 (1.09e-2) −	2.0066e-1 (2.91e-3) −	2.2296e-1 (1.36e-3) ≈	2.1727e-1 (1.05e-3) −	2.2595e-1 (1.05e-3) +	2.2280e-1 (1.29e-3)
ZXH_CF7	3	13	2.6190e-1 (9.00e-2) ≈	2.8320e-2 (5.66e-2) −	7.0418e-2 (1.04e-1) −	1.7165e-1 (1.25e-1) −	1.1377e-1 (1.12e-1) −	2.9140e-1 (8.89e-2) ≈	2.9207e-1 (7.64e-2) +	2.3999e-1 (1.11e-1)
ZXH_CF8	3	13	2.1152e-1 (5.81e-3) −	1.0386e-1 (3.34e-2) −	1.2063e-1 (1.91e-2) −	2.1263e-1 (5.15e-3) −	1.2283e-1 (1.49e-2) −	2.2296e-1 (2.93e-3) −	2.3983e-1 (8.47e-4) +	2.3083e-1 (2.12e-3)
ZXH_CF9	3	13	2.3990e-1 (9.76e-3) −	8.0970e-2 (3.67e-2) −	1.1181e-1 (3.97e-2) −	2.4880e-1 (5.50e-3) −	1.6162e-1 (6.18e-2) −	2.6303e-1 (2.74e-3) −	2.6868e-1 (1.49e-3) ≈	2.6928e-1 (1.56e-3)
ZXH_CF10	3	13	1.8661e-1 (1.01e-1) −	1.2733e-2 (2.89e-2) −	3.5459e-3 (5.36e-3) −	2.1093e-1 (1.07e-1) −	1.2441e-1 (1.05e-1) −	2.1794e-1 (1.08e-1) ≈	2.6966e-1 (1.09e-1) −	2.8353e-1 (9.58e-2)
ZXH_CF11	3	13	3.8991e-1 (8.71e-3) −	1.9864e-1 (6.11e-2) −	3.5334e-1 (1.34e-2) −	2.8437e-1 (1.85e-2) −	4.2558e-1 (2.18e-3) ≈	4.1834e-1 (3.44e-3) −	4.1681e-1 (2.89e-3) −	4.2537e-1 (2.72e-3)
ZXH_CF12	3	13	6.7025e-1 (2.02e-1) −	3.0386e-1 (1.08e-1) −	5.8553e-1 (1.03e-1) −	4.5357e-1 (2.56e-1) −	6.5299e-1 (2.46e-1) −	7.4573e-1 (6.03e-3) −	7.1742e-1 (8.46e-2) −	7.5273e-1 (2.51e-3)
ZXH_CF13	2	12	2.4196e-1 (1.10e-1) −	4.6817e-3 (1.40e-2) −	2.7546e-2 (6.94e-2) −	1.8601e-1 (1.13e-1) −	1.3589e-1 (1.25e-1) −	2.3574e-1 (1.22e-1) −	2.3806e-1 (1.12e-1) −	2.7856e-1 (1.05e-1)
ZXH_CF14	2	12	5.4203e-1 (5.07e-4) −	3.8169e-1 (1.07e-1) −	5.1251e-1 (4.30e-3) −	4.9882e-1 (9.92e-3) −	5.4317e-1 (1.18e-4) ≈	5.4114e-1 (3.36e-4) −	5.4177e-1 (6.67e-4) −	5.4320e-1 (1.38e-4)
ZXH_CF15	2	12	6.6107e-1 (2.27e-4) −	4.4797e-1 (1.43e-1) −	6.2683e-1 (2.55e-2) −	5.9186e-1 (1.01e-1) −	6.4570e-1 (5.56e-2) −	6.4283e-1 (8.01e-2) −	6.6044e-1 (2.78e-3) −	6.6173e-1 (1.68e-4)
ZXH_CF16	2	12	7.6380e-1 (7.24e-3) −	7.6813e-1 (1.59e-2) −	7.6596e-1 (2.85e-3) −	7.5343e-1 (6.85e-3) −	7.5334e-1 (1.94e-2) −	7.7809e-1 (1.65e-4) −	7.7706e-1 (5.09e-4) −	7.7822e-1 (9.22e-5)
+/ − / ≈			4/11/1	0/16/0	0/16/0	0/16/0	2/10/4	1/12/3	7/8/1	
+/ − / ≈			4/37/3	0/38/4	0/42/2	0/42/2	6/33/5	1/40/3	13/25/6	

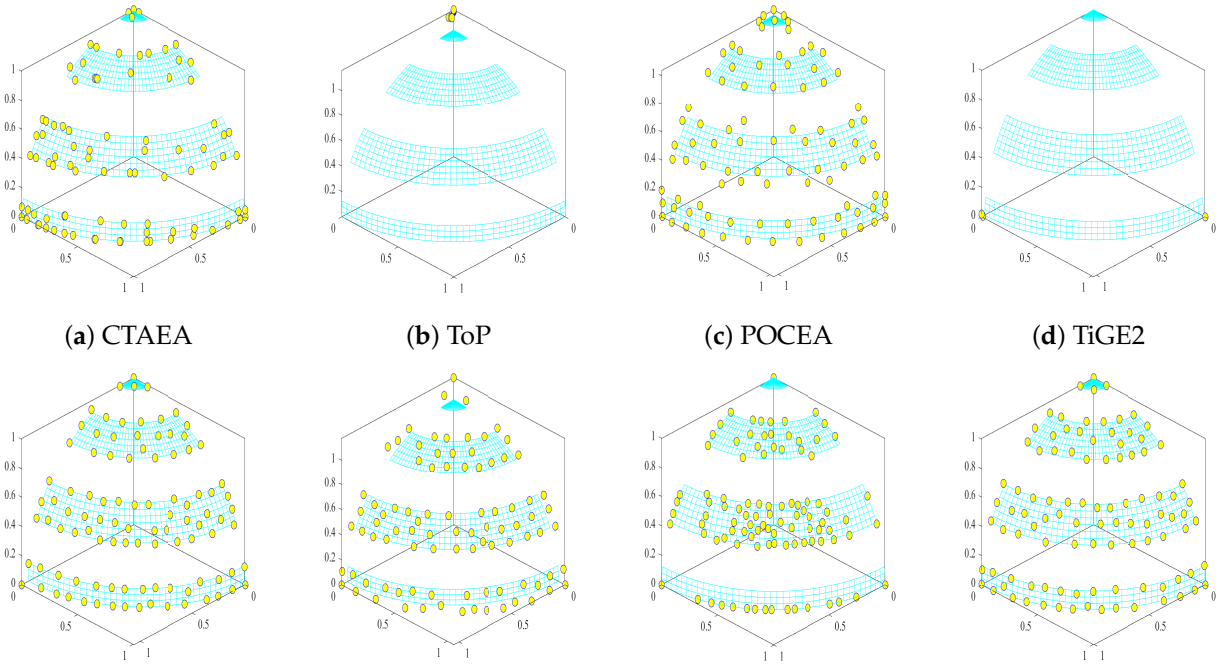
In summary of the analysis from the perspective of performance metrics, we can say the following: On 44 different benchmark test problems, CMOEA-FTR not only outperforms CTAEA, TOP, POCEA, TiGE, CMOEA-MS, CMOEA-MT, and TPCMAO by 91%, 86%, 93%, 93%, 89%, 91%, and 91%, respectively, in terms of the IGD metric, but also outperforms them by 84%, 86%, 95%, 95%, 75%, 91%, and 57%, respectively, in terms of the HV metric.

Therefore, CMOEA-FTR not only significantly outperforms its competitors in terms of the IGD metric but also excels in the HV metric compared to other competitive algorithms. Based on the analysis of the data, we can conclude that among CMOEAs, CMOEA-FTR exhibits strong competitiveness.

4.3. Analysis of the Wilcoxon Test and PF Plots

The IGD and HV data collected from 44 test problems were subjected to Wilcoxon tests. As shown in Table 3, the Wilcoxon test results compare CMOEA-FTR with seven other algorithms. It is evident that CMOEA-FTR has higher-ranked (R^+) data, with only

a small portion of data (R^-) falling behind. In Table 3, TPCMaO has an R^- IGD value of 228.0 and an HV value of 376.0, which are the highest R^- values among all compared algorithms. However, these values are still far inferior to the R^+ values of CMOEA-FTR. Additionally, we also presented the PF distribution plots on the MW test suite. In Figure 4, the yellow dots represent the distribution of solutions obtained by the algorithm on the MW8 test problem. ToP and TiGE2 did not find PF, while POCEA and CMOEMT found PF, but only a portion of the solutions are on the PF. Although most solutions of CTAEA and CMOEA_MS are on the PF, their distributions are uneven and relatively sparse. In contrast, CMOEA-FTR not only has all solutions on the PF but also distributes them evenly and densely. Considering the Wilcoxon test results in Table 3 and the PF distribution plots on the MW test suite, CMOEA-FTR demonstrates strong competitiveness compared to other algorithms.



(**a**) CTAEA (**b**) ToP (**c**) POCEA (**d**) TiGE2

(**e**) CMOEA_M (**f**) CMOEMT (**g**) TPCMaO (**h**) CMOEA-FTR

Figure 4. Pareto front (PF) plot obtained for MW8 test problem.

Table 3. IGD and HV Wilcoxon test statistics derived from 44 test questions.

CMOEA-FTR vs.	IGD			HV		
	R^+	R^-	*p*-Value	R^+	R^-	*p*-Value
CTAEA	942.0	48.0	0	921.0	69.0	0.000001
ToP	903.0	−2.0	0	903.0	−2.0	0
POCEA	972.0	18.0	0	981.0	9.0	0
TiGE2	959.0	31.0	0	988.0	2.0	0
CMOEA-MS	886.0	104.0	0.000005	894.5	95.5	0.000003
CMOEMT	944.0	46.0	0	903.0	43.0	0
TPCMaO	762.0	228.0	0.001798	614.0	376.0	0.146566

4.4. Application in Real-World Test Cases

In this section, eight algorithms are compared across 16 real-world test cases. Since the true PF cannot be obtained for the applied cases, the HV metric derived from the reference algorithms is used for analysis. As shown clearly in Table 4, out of 16 real-world application cases, CMOEA-FTR achieved the best performance in 11 cases, with only 4 cases performing worse than the competitors. Further explanation shows that the feedback tracking strategy

not only has the ability to expand solutions but also possesses strong adaptability. Therefore, CMOEA-FTR demonstrates strong general applicability in real-world scenarios.

Table 4. Statistical outcomes (avg ± std) of HV values for eight CMOEAs on RWMOP problems.

Problem	*M*	*D*	CTAEA	ToP	POCEA	TiGE2	CMOEA_MS	CMOEMT	TPCMaO	CMOEA_TDE
RWMOP1	2	4	6.0664e-1 (1.02e-3) −	6.0781e-1 (3.75e-4) −	5.9206e-1 (5.28e-3) −	5.4586e-1 (2.37e-2) −	7.0686e-1 (1.46e-1) +	6.0677e-1 (5.07e-4) −	5.9896e-1 (4.24e-2) −	6.0901e-1 (1.72e-4)
RWMOP2	2	5	2.5408e-1 (1.82e-1) −	3.9279e-1 (7.10e-4) −	1.6272e-1 (1.12e-1) −	2.4040e-1 (1.48e-1) −	3.1613e-1 (1.17e-1) −	3.9290e-1 (4.15e-5) −	3.4714e-1 (6.61e-2) −	3.9300e-1 (1.04e-5)
RWMOP3	2	3	8.8768e-1 (1.21e-2) −	9.0175e-1 (2.26e-4) −	2.3952e-1 (1.66e-1) −	8.9583e-1 (1.39e-3) −	8.6370e-1 (6.49e-3) −	8.9847e-1 (6.65e-4) −	8.9853e-1 (6.87e-4) −	9.0248e-1 (1.07e-4)
RWMOP4	2	4	8.5106e-1 (1.25e-2) −	8.6267e-1 (2.21e-4) ≈	3.4838e-2 (1.43e-1) −	8.3175e-1 (6.68e-3) −	8.0111e-1 (2.57e-2) −	8.5661e-1 (1.41e-3) −	8.6055e-1 (1.74e-3) −	8.6240e-1 (1.49e-3)
RWMOP5	2	4	4.3173e-1 (1.64e-3) −	4.3452e-1 (1.02e-4) −	4.2557e-1 (1.61e-3) −	4.2078e-1 (4.95e-3) −	4.2090e-1 (2.52e-3) −	4.3450e-1 (1.68e-4) −	3.9596e-1 (1.43e-2) −	4.3516e-1 (7.34e-5)
RWMOP6	2	7	2.4217e-1 (3.89e-2) −	2.7702e-1 (3.56e-4) −	2.7421e-1 (1.21e-3) −	2.7086e-1 (1.37e-3) −	2.7729e-1 (8.98e-6) +	2.7642e-1 (1.06e-4) −	2.7674e-1 (2.45e-4) −	2.7722e-1 (1.38e-5)
RWMOP7	2	4	4.8391e-1 (2.44e-4) −	4.8443e-1 (5.76e-5) −	4.8014e-1 (1.34e-3) −	4.2868e-1 (3.61e-2) −	4.8414e-1 (4.41e-4) −	4.8461e-1 (3.55e-5) −	4.8312e-1 (1.02e-3) −	4.8468e-1 (3.62e-5)
RWMOP8	3	7	2.6099e-2 (2.95e-5) −	2.5770e-2 (1.09e-4) −	1.7120e-2 (3.29e-3) −	2.0457e-2 (2.47e-4) −	2.6099e-2 (3.12e-4) ≈	2.5863e-2 (5.83e-5) −	2.5423e-2 (2.00e-4) −	2.6141e-2 (4.09e-5)
RWMOP9	2	4	4.0882e-1 (4.77e-4) −	4.0929e-1 (1.30e-4) −	4.0634e-1 (1.24e-3) −	3.9604e-1 (3.92e-3) −	4.0859e-1 (2.23e-4) −	4.0952e-1 (1.22e-4) −	4.0865e-1 (5.60e-4) −	4.0995e-1 (8.87e-5)
RWMOP10	2	2	8.4173e-1 (4.34e-3) −	8.4736e-1 (1.20e-4) −	8.3907e-1 (3.51e-3) −	8.4108e-1 (2.75e-3) −	8.3874e-1 (7.53e-4) −	8.4206e-1 (1.85e-3) −	8.3753e-1 (4.25e-3) −	8.4751e-1 (3.83e-5)
RWMOP11	5	3	9.4576e-2 (9.78e-4) −	8.6757e-2 (2.75e-3) −	5.7791e-2 (9.80e-3) −	9.5972e-2 (5.60e-4) −	8.9004e-2 (4.14e-3) −	9.0453e-2 (2.45e-3) −	3.5918e-2 (6.76e-3) −	9.7353e-2 (6.60e-4)
RWMOP12	2	4	5.4770e-1 (7.78e-3) −	5.6025e-1 (3.26e-4) +	3.3342e-1 (1.53e-2) −	5.4944e-1 (2.79e-3) −	4.6522e-1 (5.49e-2) −	5.5558e-1 (1.30e-3) −	5.6145e-1 (1.75e-4) +	5.6009e-1 (4.15e-3)
RWMOP13	3	7	8.6644e-2 (6.45e-4) −	8.7701e-2 (1.20e-4) −	6.5544e-2 (1.30e-2) −	8.5329e-2 (7.18e-4) −	8.2105e-2 (2.30e-3) −	8.7082e-2 (1.93e-4) −	8.7364e-2 (7.69e-4) −	8.8089e-2 (7.77e-5)
RWMOP14	2	5	6.1759e-1 (8.33e-4) −	6.1780e-1 (1.58e-4) −	7.3142e-2 (2.63e-2) −	5.0699e-1 (5.29e-2) −	3.8999e-1 (1.17e-1) −	6.1681e-1 (4.84e-4) −	6.1559e-1 (1.16e-3) −	6.1885e-1 (1.10e-4)
RWMOP15	2	3	5.3629e-1 (1.34e-2) −	5.4360e-1 (1.87e-5) +	5.2446e-1 (5.30e-3) −	5.2459e-1 (3.25e-3) −	5.4335e-1 (2.33e-4) −	5.4332e-1 (2.52e-4) −	5.4242e-1 (9.69e-4) −	5.4354e-1 (3.97e-5)
RWMOP16	2	2	7.6263e-1 (3.75e-4) −	7.6373e-1 (1.26e-4) −	7.2909e-1 (5.04e-3) −	7.5067e-1 (3.62e-3) −	7.5541e-1 (1.35e-3) −	7.6242e-1 (2.64e-4) −	7.6210e-1 (5.17e-4) −	7.6418e-1 (3.93e-5)
ing+/ − / ≈			0/16/0	2/13/1	0/16/0	0/16/0	2/13/1	0/16/0	1/15/0	

In the realm of intelligent manufacturing, the CMOEA-FTR algorithm proves highly effective in tackling multi-objective optimization challenges within production processes, including minimizing energy usage, boosting efficiency, and refining process workflows. By enhancing resource allocation strategies, this algorithm not only cuts down on production costs but also increases the adaptability and responsiveness of production lines, enabling them to swiftly adjust to fluctuating market demands. This approach is particularly beneficial during the transition from traditional to smart manufacturing, offering innovative solutions that can propel the industry's modernization and transformation.

4.5. Verification and Analysis of CMOEA-FTR Innovations

In this part of the study, we verify the innovations of CMOEA-FTR. The superiority of CMOEA-FTR is substantiated by comparing it with five designed variants (i.e., CMOEA-FTR1-5). The specific designs are as follows:

(1) In CMOEA-FTR1: Remove the two-stage framework.
(2) In CMOEA-FTR2: Remove all diversity ranking, convergence ranking, and fitness evaluation mechanisms, and replace them with standard non-dominated sorting.
(3) In CMOEA-FTR3: Remove the adaptive feedback scaling constraint relaxation mechanism in the first stage.
(4) In CMOEA-FTR4: Remove the elite mating pool selection process for parent selection and replace it with binary tournament selection.
(5) In CMOEA-FTR5: Remove the elite environmental selection in the second stage and replace it with standard environmental selection.

From the IGD metrics in Table 5, it can be seen that CMOEA-FTR1 not only fails to find feasible solutions on the MW1 test problem but also performs worse than CMOEA-FTR on 11 test problems. This indicates that the new two-stage framework has achieved very good results. CMOEA-FTR outperforms CMOEA-FTR2 on eight test problems, indicating that the diversity ranking, convergence ranking, and fitness evaluation mechanisms have strong competitiveness in solution selection. CMOEA-FTR3 performs worse than CMOEA-FTR on 10 test problems, indicating that CMOEA-FTR with the added adaptive feedback scaling constraint relaxation mechanism exhibits strong competitiveness. Although CMOEA-FTR4 achieves the best results on MW1 and MW4, it performs worse than CMOEA-FTR on 11 test problems, which supports the effectiveness of the designed elite mating pool selection process for parent selection. Finally, CMOEA-FTR5 fails to find feasible solutions

on three test problems, significantly impacting the algorithm's efficiency. Additionally, it performs worse than CMOEA-FTR on 10 test problems, which validates the superiority of the elite environmental selection.

Additionally, from the HV values in Table 6, it can be seen that CMOEA-FTR outperforms the other five variants on 9, 7, 9, 10, and 10 test problems, further validating the strong effectiveness of our proposed innovations and confirming the strong competitiveness of CMOEA-FTR.

Table 5. IGD results (avg ± std) obtained for CMOEA-FTR1, CMOEA-FTR2, CMOEA-FTR3, CMOEA-FTR4, CMOEA-FTR5, and CMOEA-FTR on MW benchmark problems.

Problem	*M*	*D*	CMOEA-FTR1	CMOEA-FTR2	CMOEA-FTR3	CMOEA-FTR4	CMOEA-FTR5	CMOEA-FTR
MW1	2	15	NaN (NaN)	1.6233e-3 (1.31e-5) ≈	9.5843e-3 (8.51e-3) −	1.6191e-3 (1.17e-5) +	4.0991e-3 (2.09e-4) −	1.6273e-3 (6.62e-6)
MW2	2	15	6.1112e-2 (3.45e-2) −	4.1376e-3 (5.17e-4) −	5.4254e-3 (2.35e-3) ≈	1.0918e-1 (8.83e-2) −	4.5838e-3 (2.31e-3) −	3.9112e-3 (4.37e-5)
MW3	2	15	4.9885e-3 (2.11e-4) +	5.1348e-3 (1.54e-4) ≈	6.4837e-3 (7.91e-4) −	5.3757e-3 (4.87e-4) −	5.2536e-2 (1.41e-3) −	5.1205e-3 (1.78e-4)
MW4	3	15	2.2259e-1 (3.40e-1) −	4.2046e-2 (3.71e-4) ≈	4.7080e-2 (2.87e-3) −	4.1440e-2 (4.50e-4) +	4.4092e-2 (1.21e-3) −	4.1997e-2 (4.90e-4)
MW5	2	15	4.4876e-1 (5.20e-1) −	9.4445e-4 (6.88e-4) −	6.0439e-3 (3.10e-3) −	3.6838e-1 (3.66e-1) −	3.2551e-1 (2.11e-1) −	4.7347e-4 (9.08e-5)
MW6	2	15	2.5330e-1 (2.17e-1) −	2.7355e-3 (2.48e-5) ≈	3.8659e-3 (2.38e-3) ≈	4.4060e-1 (4.28e-1) −	8.0864e-3 (8.33e-3) −	4.6368e-3 (6.65e-3)
MW7	2	15	6.0838e-3 (5.70e-4) −	7.3633e-3 (1.20e-3) −	5.8586e-3 (6.68e-4) −	2.9735e-2 (9.93e-2) −	2.0582e-1 (2.95e-3) −	5.1892e-3 (3.30e-4)
MW8	3	15	6.1104e-2 (1.31e-2) −	4.6267e-2 (1.60e-2) ≈	4.3111e-2 (8.02e-4) ≈	1.6217e-1 (2.11e-1) −	5.9729e-2 (3.46e-3) −	4.3044e-2 (6.03e-4)
MW9	2	15	3.3553e-1 (3.87e-1) −	9.6737e-3 (2.30e-3) −	2.0669e-2 (5.62e-3) −	9.3673e-3 (1.74e-3) −	NaN (NaN)	4.8779e-3 (3.00e-4)
MW10	2	15	2.6752e-1 (2.15e-1) −	4.3197e-3 (2.31e-3) −	5.2628e-3 (3.96e-3) ≈	2.4411e-1 (2.07e-1) −	3.5212e-2 (8.15e-2) −	3.6954e-3 (1.40e-3)
MW11	2	15	6.4730e-3 (2.37e-4) −	6.9349e-3 (2.81e-4) −	6.6709e-3 (2.64e-4) −	7.2554e-3 (4.20e-4) −	NaN (NaN)	6.1095e-3 (1.61e-4)
MW12	2	15	1.6635e-1 (2.65e-1) −	5.0744e-3 (6.13e-4) −	6.1396e-3 (2.32e-3) −	4.9612e-3 (1.75e-4) −	NaN (NaN)	4.7527e-3 (8.47e-5)
MW13	2	15	7.4532e-1 (7.02e-1) −	4.2754e-2 (3.51e-2) −	3.9268e-2 (2.63e-2) −	5.0102e-1 (4.68e-1) −	1.1160e-1 (1.24e-2) −	1.2653e-2 (6.04e-3)
MW14	3	15	9.7064e-2 (1.64e-3) ≈	9.7173e-2 (1.37e-3) ≈	1.6310e-1 (1.27e-1) −	9.7874e-2 (1.60e-3) ≈	9.6449e-2 (3.18e-3) ≈	9.7846e-2 (1.69e-3)
ing+/ − / ≈			1/11/1	0/8/6	0/10/4	2/11/1	0/10/1	

Table 6. HV results (avg ± std) obtained for CMOEA-FTR1, CMOEA-FTR2, CMOEA-FTR3, CMOEA-FTR4, CMOEA-FTR5, and CMOEA-FTR on MW benchmark problems.

Problem	*M*	*D*	CMOEA-FTR1	CMOEA-FTR2	CMOEA-FTR3	CMOEA-FTR4	CMOEA-FTR5	CMOEA-FTR
MW1	2	15	NaN (NaN)	4.8999e-1 (3.70e-5) ≈	4.7391e-1 (1.36e-2) −	4.9005e-1 (4.50e-5) +	4.8523e-1 (7.51e-4) −	4.8996e-1 (4.68e-5)
MW2	2	15	4.9687e-1 (4.24e-2) −	5.8179e-1 (6.66e-4) −	5.7989e-1 (3.75e-3) ≈	4.4050e-1 (9.92e-2) −	5.8121e-1 (3.61e-3) −	5.8209e-1 (6.78e-5)
MW3	2	15	5.4405e-1 (3.82e-4) ≈	5.4406e-1 (3.44e-4) ≈	5.4157e-1 (1.50e-3) −	5.4378e-1 (8.40e-4) ≈	5.3307e-1 (1.78e-3) −	5.4390e-1 (2.97e-4)
MW4	3	15	6.4828e-1 (3.18e-1) −	8.3912e-1 (8.57e-4) ≈	8.3056e-1 (3.92e-3) −	8.4070e-1 (7.11e-4) +	8.3859e-1 (1.29e-3) −	8.3943e-1 (7.34e-4)
MW5	2	15	1.5677e-1 (1.54e-1) −	3.2409e-1 (2.86e-4) −	3.2093e-1 (1.65e-3) −	2.0786e-1 (1.14e-1) −	2.1769e-1 (4.70e-2) −	3.2440e-1 (6.63e-5)
MW6	2	15	1.9102e-1 (7.32e-2) −	3.2851e-1 (1.65e-5) ≈	3.2767e-1 (1.96e-3) +	1.4637e-1 (1.10e-1) −	3.2042e-1 (1.31e-2) −	3.2569e-1 (9.68e-3)
MW7	2	15	4.1122e-1 (6.28e-4) ≈	4.1132e-1 (4.47e-4) ≈	4.1067e-1 (9.45e-4) ≈	4.0188e-1 (3.70e-2) −	3.3991e-1 (1.93e-3) −	4.1109e-1 (6.60e-4)
MW8	3	15	4.9235e-1 (2.83e-2) −	5.4243e-1 (3.65e-2) ≈	5.5088e-1 (3.75e-3) ≈	3.9088e-1 (1.37e-1) −	5.2650e-1 (1.08e-2) −	5.5056e-1 (2.26e-3)
MW9	2	15	2.1252e-1 (1.77e-1) −	3.8642e-1 (4.68e-3) −	3.7318e-1 (5.68e-3) −	3.8626e-1 (2.92e-3) −	NaN (NaN)	3.9567e-1 (1.97e-3)
MW10	2	15	2.9914e-1 (9.44e-2) −	4.5386e-1 (1.43e-3) −	4.5139e-1 (6.34e-3) ≈	3.1178e-1 (9.46e-2) −	4.3214e-1 (4.92e-2) −	4.5418e-1 (2.69e-3)
MW11	2	15	4.4734e-1 (3.20e-4) ≈	4.4680e-1 (2.52e-4) −	4.4694e-1 (3.54e-4) −	4.4660e-1 (3.93e-4) −	NaN (NaN)	4.4751e-1 (2.46e-4)
MW12	2	15	4.5246e-1 (2.35e-1) −	6.0364e-1 (1.10e-3) −	6.0191e-1 (3.52e-3) −	6.0406e-1 (4.73e-4) −	NaN (NaN)	6.0470e-1 (3.17e-4)
MW13	2	15	2.2737e-1 (1.59e-1) −	4.7074e-1 (1.05e-2) −	4.6117e-1 (1.15e-2) −	2.8411e-1 (1.21e-1) −	4.5883e-1 (3.45e-3) −	4.7537e-1 (4.41e-3)
MW14	3	15	4.7119e-1 (1.52e-3) ≈	4.7041e-1 (1.45e-3) ≈	4.4554e-1 (4.97e-2) −	4.7062e-1 (1.61e-3) ≈	4.7392e-1 (1.25e-3) +	4.7047e-1 (1.20e-3)
ing+/ − / ≈			0/9/4	0/7/7	1/9/4	2/10/2	1/10/0	

4.6. Analysis of CMOEA-FTR and Competitor Algorithms

In this paper, to validate the proposed CMOEA-FTR optimizer and its superiority over previous state-of-the-art methods, the seven most advanced CMOEAs were selected as competitors and compared through experiments on the MW, LIRCMOP, and ZXH_CF test suites. Based on the results of the IGD and HV metrics, although CMOEA-FTR may not outperform its competitors on certain test problems, it shows superior performance over its competitors when considering the 44 test problems across the three test suites.

Next, we conducted comparative experiments on 16 real-world RWMOP cases, where CMOEA-FTR clearly demonstrated strong practical applicability. When facing nonlinear case problems, CMOEA-FTR achieved the best values compared to its competitors. Finally,

we performed ablation experiments to validate the superiority of the feedback tracking optimizer. From the ablation data in Tables 5 and 6, it is evident that the local variants of CMOEA-FTR perform worse than CMOEA-FTR, further validating its superiority.

The competing algorithms used are recent academic landmark works published in renowned journals, and the platform PlatEMO employed is an open-source public testing and training platform in this research direction. The obtained IGD and HV test results are highly persuasive. Therefore, based on the above analysis, the proposed CMOEA-FTR optimizer outperforms previous state-of-the-art algorithms.

5. Conclusions

To address CMOPs with different characteristics, this paper proposes a CMOEA based on feedback tracking constraint relaxation, referred to as CMOEA-FTR. First Phase: An adaptive feedback scaling constraint relaxation mechanism is designed to introduce more infeasible solutions, which are stored in an archive and continuously updated as the algorithm iterates. This enhances the ability to explore unknown regions, making the CPF infinitely close to the UPF. During the stretching of the constraint boundaries, a fitness evaluation mechanism is employed to eliminate redundant solutions, maintaining a balance between diversity and convergence. Additionally, in the elite mating pool, a new constraint dominance principle is designed to select high-quality parents. Second Phase: All constraint relaxation mechanisms are halted, and an elite environmental selection is performed on the candidate solutions to maintain a balance between convergence and diversity. The experimental results demonstrate that CMOEA-FTR not only achieved excellent performance on benchmark test problems but also exhibited strong competitiveness in commonly used real-world cases.

In future research, we will explore how to make the algorithm more stable and avoid extreme situations. Additionally, extending this algorithm to dynamic and many-objective problems is worth investigating. Applying it to complex real-world problems is also a potential future task.

Author Contributions: Conceptualization, Y.L. and J.C. (Junming Chen); data curation, J.C. (Junming Chen) and J.C. (Jialin Cai); formal analysis, J.C. (Junming Chen); funding acquisition, J.C. (Jialin Cai); investigation, J.C. (Junming Chen) and J.C. (Jialin Cai); methodology, Y.L. and J.C. (Junming Chen); project administration, J.C. (Jialin Cai); resources, J.C. (Jialin Cai); software, J.C. (Junming Chen); supervision, J.C. (Junming Chen) and J.C. (Jialin Cai); validation, J.C. (Junming Chen); visualization, J.C. (Junming Chen); writing—original draft, Y.L., J.C. (Junming Chen), Y.C., H.Z., and J.C. (Jialin Cai); writing—review and editing, Y.L., J.C. (Junming Chen), Y.C., H.Z., and J.C. (Jialin Cai). All authors have read and agreed to the published version of the manuscript.

Funding: This research received no external funding.

Data Availability Statement: The raw data supporting the conclusions of this article will be made available by the authors on request.

Conflicts of Interest: The authors declare no conflicts of interest.

References

1. Yang, Y.; Yan, B.; Kong, X.; Zhao, J. A double auxiliary optimization constrained multi-objective evolutionary algorithm. *Math. Comput. Simul.* **2024**, *220*, 567–579. [CrossRef]
2. Zhang, H.; Yue, D.; Dou, C.; Hancke, G.P. PBI based multi-objective optimization via deep reinforcement elite learning strategy for micro-grid dispatch with frequency dynamics. *IEEE Trans. Power Syst.* **2022**, *38*, 488–498. [CrossRef]
3. Xu, X.; Lin, Z.; Li, X.; Shang, C.; Shen, Q. Multi-objective robust optimisation model for MDVRPLS in refined oil distribution. *Int. J. Prod. Res.* **2022**, *60*, 6772–6792. [CrossRef]

4. Zhu, M.; Arabi Nowdeh, S.; Daskalopulu, A. An Improved Human-Inspired Algorithm for Distribution Network Stochastic Reconfiguration Using a Multi-Objective Intelligent Framework and Unscented Transformation. *Mathematics* **2023**, *11*, 3658. [CrossRef]
5. Xia, J.Y.; Li, S.; Huang, J.J.; Yang, Z.; Jaimoukha, I.M.; Gündüz, D. Metalearning-based alternating minimization algorithm for nonconvex optimization. *IEEE Trans. Neural Netw. Learn. Syst.* **2022**, *34*, 5366–5380. [CrossRef]
6. Nowdeh, S.A.; Davoudkhani, I.F.; Moghaddam, M.H.; Najmi, E.S.; Abdelaziz, A.Y.; Ahmadi, A.; Razavi, S.E.; Gandoman, F.H. Fuzzy multi-objective placement of renewable energy sources in distribution system with objective of loss reduction and reliability improvement using a novel hybrid method. *Appl. Soft Comput.* **2019**, *77*, 761–779. [CrossRef]
7. Ming, F.; Gong, W.; Zhen, H.; Li, S.; Wang, L.; Liao, Z. A simple two-stage evolutionary algorithm for constrained multi-objective optimization. *Knowl.-Based Syst.* **2021**, *228*, 107263. [CrossRef]
8. Tian, Y.; Zhang, T.; Xiao, J.; Zhang, X.; Jin, Y. A coevolutionary framework for constrained multiobjective optimization problems. *IEEE Trans. Evol. Comput.* **2020**, *25*, 102–116. [CrossRef]
9. Li, K.; Chen, R.; Fu, G.; Yao, X. Two-archive evolutionary algorithm for constrained multiobjective optimization. *IEEE Trans. Evol. Comput.* **2018**, *23*, 303–315. [CrossRef]
10. Xu, C.; Zhou, X.; Lin, X.; Peng, W.; Zhang, C. Automated optimization for steel mold of precast components based on multi-objective evolutionary algorithm. *J. Constr. Steel Res.* **2024**, *221*, 108914. [CrossRef]
11. Tian, Y.; Zhang, Y.; Su, Y.; Zhang, X.; Tan, K.C.; Jin, Y. Balancing objective optimization and constraint satisfaction in constrained evolutionary multiobjective optimization. *IEEE Trans. Cybern.* **2021**, *52*, 9559–9572. [CrossRef] [PubMed]
12. Wang, J.; Liang, G.; Zhang, J. Cooperative differential evolution framework for constrained multiobjective optimization. *IEEE Trans. Cybern.* **2018**, *49*, 2060–2072. [CrossRef] [PubMed]
13. Li, Y.; Feng, X.; Yu, H. A constrained multiobjective evolutionary algorithm with the two-archive weak cooperation. *Inf. Sci.* **2022**, *615*, 415–430. [CrossRef]
14. Sun, J.; Zhang, Z.; Zhang, G.; Huang, Z. Multi-objective evolutionary algorithm based flexible assembly job-shop rescheduling with component sharing for order insertion. *Comput. Oper. Res.* **2024**, *169*, 106744. [CrossRef]
15. Wang, J.; Li, Y.; Zhang, Q.; Zhang, Z.; Gao, S. Cooperative multiobjective evolutionary algorithm with propulsive population for constrained multiobjective optimization. *IEEE Trans. Syst. Man Cybern. Syst.* **2021**, *52*, 3476–3491. [CrossRef]
16. Deb, K.; Pratap, A.; Agarwal, S.; Meyarivan, T. A fast and elitist multiobjective genetic algorithm: NSGA-II. *IEEE Trans. Evol. Comput.* **2002**, *6*, 182–197. [CrossRef]
17. Oyama, A.; Shimoyama, K.; Fujii, K. New constraint-handling method for multi-objective and multi-constraint evolutionary optimization. *Trans. Jpn. Soc. Aeronaut. Space Sci.* **2007**, *50*, 56–62. [CrossRef]
18. Chen, Q.; Ding, J.; Yang, S.; Chai, T. A novel evolutionary algorithm for dynamic constrained multiobjective optimization problems. *IEEE Trans. Evol. Comput.* **2019**, *24*, 792–806. [CrossRef]
19. Jan, M.A.; Khanum, R.A. A study of two penalty-parameterless constraint handling techniques in the framework of MOEA/D. *Appl. Soft Comput.* **2013**, *13*, 128–148. [CrossRef]
20. Fan, Z.; Li, W.; Cai, X.; Hu, K.; Lin, H.; Li, H. Angle-based constrained dominance principle in MOEA/D for constrained multi-objective optimization problems. In Proceedings of the 2016 IEEE Congress on Evolutionary Computation (CEC), Vancouver, BC, Canada, 24–29 July 2016; IEEE: Piscataway, NJ, USA, 2016; pp. 460–467.
21. Ray, T.; Tai, K.; Seow, K.C. Multiobjective design optimization by an evolutionary algorithm. *Eng. Optim.* **2001**, *33*, 399–424. [CrossRef]
22. Young, N. Blended ranking to cross infeasible regions in constrainedmultiobjective problems. In Proceedings of the International Conference on Computational Intelligence for Modelling, Control and Automation and International Conference on Intelligent Agents, Web Technologies and Internet Commerce (CIMCA-IAWTIC'06), Vienna, Austria, 28–30 November 2005; IEEE: Piscataway, NJ, USA, 2005; Volume 2, pp. 191–196.
23. Woldesenbet, Y.G.; Yen, G.G.; Tessema, B.G. Constraint handling in multiobjective evolutionary optimization. *IEEE Trans. Evol. Comput.* **2009**, *13*, 514–525. [CrossRef]
24. Peng, C.; Liu, H.L.; Gu, F. An evolutionary algorithm with directed weights for constrained multi-objective optimization. *Appl. Soft Comput.* **2017**, *60*, 613–622. [CrossRef]
25. Wang, F.; Huang, M.; Yang, S.; Wang, X. Penalty and prediction methods for dynamic constrained multi-objective optimization. *Swarm Evol. Comput.* **2023**, *80*, 101317. [CrossRef]
26. Fan, Z.; Li, W.; Cai, X.; Li, H.; Wei, C.; Zhang, Q.; Deb, K.; Goodman, E. Push and pull search for solving constrained multi-objective optimization problems. *Swarm Evol. Comput.* **2019**, *44*, 665–679. [CrossRef]
27. Liu, Z.Z.; Wang, Y. Handling constrained multiobjective optimization problems with constraints in both the decision and objective spaces. *IEEE Trans. Evol. Comput.* **2019**, *23*, 870–884. [CrossRef]
28. He, C.; Cheng, R.; Tian, Y.; Zhang, X.; Tan, K.C.; Jin, Y. Paired offspring generation for constrained large-scale multiobjective optimization. *IEEE Trans. Evol. Comput.* **2020**, *25*, 448–462. [CrossRef]

29. Ma, H.; Wei, H.; Tian, Y.; Cheng, R.; Zhang, X. A multi-stage evolutionary algorithm for multi-objective optimization with complex constraints. *Inf. Sci.* **2021**, *560*, 68–91. [CrossRef]
30. Qiao, K.; Liang, J.; Yu, K.; Yue, C.; Lin, H.; Zhang, D.; Qu, B. Evolutionary constrained multiobjective optimization: Scalable high-dimensional constraint benchmarks and algorithm. *IEEE Trans. Evol. Comput.* **2023**, *28*, 65–979. [CrossRef]
31. Tian, Y.; Shi, Z.; Zhang, Y.; Zhang, L.; Zhang, H.; Zhang, X. Solving optimal power flow problems via a constrained many-objective co-evolutionary algorithm. *Front. Energy Res.* **2023**, *11*, 1293193. [CrossRef]
32. Cao, J.; Yan, Z.; Chen, Z.; Zhang, J. A coevolutionary constrained multi-objective algorithm with a learning constraint boundary. *Appl. Soft Comput.* **2023**, *148*, 110845. [CrossRef]
33. Chen, J.; Zhang, K.; Zeng, H.; Yan, J.; Dai, J.; Dai, Z. Adaptive Constraint Relaxation-Based Evolutionary Algorithm for Constrained Multi-Objective Optimization. *Mathematics* **2024**, *12*, 3075. [CrossRef]
34. Do, Q.B. A non-dominated discrete differential evolution for fuel loading pattern optimization of a nuclear research reactor. *Kerntechnik* **2023**, *88*, 687–696. [CrossRef]
35. Zhou, Y.; Zhu, M.; Wang, J.; Zhang, Z.; Xiang, Y.; Zhang, J. Tri-goal evolution framework for constrained many-objective optimization. *IEEE Trans. Syst. Man Cybern. Syst.* **2018**, *50*, 3086–3099. [CrossRef]
36. Ming, F.; Gong, W.; Wang, L.; Gao, L. Constrained multiobjective optimization via multitasking and knowledge transfer. *IEEE Trans. Evol. Comput.* **2022**, *28*, 77–89. [CrossRef]
37. Deb, K.; Agrawal, R.B. Simulated binary crossover for continuous search space. *Complex Syst.* **1995**, *9*, 115–148.
38. Tian, Y.; Zhu, W.; Zhang, X.; Jin, Y. A practical tutorial on solving optimization problems via PlatEMO. *Neurocomputing* **2023**, *518*, 190–205. [CrossRef]

Disclaimer/Publisher's Note: The statements, opinions and data contained in all publications are solely those of the individual author(s) and contributor(s) and not of MDPI and/or the editor(s). MDPI and/or the editor(s) disclaim responsibility for any injury to people or property resulting from any ideas, methods, instructions or products referred to in the content.